THE WxxxE EFFECTOR MAP FUNCTIONS AS A POTENT AND SPECIFIC GUANINE NUCLEOTIDE EXCHANGE FACTOR FOR CDC42

APPROVED BY SUPERVISORY COMMITTEE

_____

Neal Alto, Ph.D.

_____

David Hendrixson, Ph.D.

_____

Nicholas Conrad, Ph.D.

DEDICATION

I dedicate this work to my parents, James and Valerie Wallenfang, the foundation for all of my successes, and my little sister, Katie Wallenfang. I would also like to dedicate it to my mentor Neal Alto for his patient and generous guidance during this chapter of my education. Finally, all this work was done in loving memory of my friend Carl Kemner.

THE WxxxE EFFECTOR MAP FUNCTIONS AS A POTENT AND SPECIFIC GUANINE NUCLEOTIDE EXCHANGE FACTOR FOR CDC42

by

ADAM JAMES WALLENFANG

THESIS

Presented to the Faculty of the Graduate School of Biomedical Sciences

The University of Texas Southwestern Medical Center at Dallas

In Partial Fullfillment of the Requirements

For the Degree of

MASTER OF SCIENCE

The University of Texas Southwestern Medical Center at Dallas

Dallas, Texas

June, 2009

THE WxxxE EFFECTOR MAP FUNCTIONS AS A POTENT AND SPECIFIC GUANINE NUCLEOTIDE EXCHANGE FACTOR FOR CDC42

Publication No_____

Adam Wallenfang

The University of Texas Southwestern Medical Center at Dallas, 2009

Supervising Professor: Neal M. Alto, Ph.D.

Many gram negative bacterial pathogens utilize a type three secretion system (TTSS) in order to infect eukaryotic cells. A TTSS looks and acts like a molecular syringe, allowing bacteria to inject effector proteins directly into the host cell cytoplasm. These effectors commandeer and manipulate host signaling pathways to support the lifecycle of the particular pathogen. Common targets for these effectors are small GTPases, particularly those controlling the actin cytoskeletal architecture.

GTPases are molecular switches found within a diverse consortium of eukaryotic signaling pathways. As their name denotes, the primary enzymatic activity of GTPases is the conversion of bound guanine triphosphate (GTP) to guanine diphosphate (GDP) via the hydrolysis of the gamma phosphate. The oscillation between the “off” or GDP-bound form and the “on” or GTP-bound form is facilitated by the action of GTPase activating factors (GAPs) and Guanine Nucleotide Exchange Factors (GEFs). GAPs accelerate the intrinsic catalytic activity of the GTPase to physiologically relevant levels and lead to the rapid inactivation of a GTPase.

GEFs conformationally eject bound GDP from inactivated GTPases allowing the binding of GTP and the activation GTPases and downstream pathways. Lipid modifications also allow GTPase activity to be localized within a eukaryotic cell. Their switch-like function, preeminence in signaling, and localized activity make GTPases great targets for bacterial effectors.

Several members of a multispecies group of effectors known as the WxxxE family appear to mimic certain Rho GTPases. The WxxxE family is defined by the motif of an invariant tryptophan and glutamic acid separated by three variable residues. Given the frequent incidence of horizontal gene transfer in bacterial evolution, it is not surprising that such a family might exist between TTSS pathogens, but this family does not contain a high level of homology besides the titular motif. Upon expression in eukaryotic cells, some WxxxE effectors have been shown to produce phenotypes identical to those seen when over-expressing certain GTPases. For example, the *Shigella* effectors IpgB1 and IpgB2 produce Rac1-characteristic lamellipodia and RhoA-characteristic actin stress fibers. The enteropathogenic and enterohaemorrhagic *E. coli* effector Map produces filipodia similar to Cdc42.

This study demonstrates that the enzymatic activity of EHEC O157:H7 Map as a specific GEF for cellular Cdc42. Structure/function studies were used to identify key residues and protein regions of *Shigella* IpgB2, *E. coli* Map, and *Salmonella* SifA that suggests that the WxxxE family functions through a SopE-like GEF biochemical activity. We propose that the WxxxE family members physically couple GTPase activation to downstream signaling pathways via a highly evolved pathogenic mechanism. These findings also suggest the possibility of GAP or GAP-like bacterial effectors counter to the WxxxEs over the course of pathogenesis, which is briefly explored in the EHEC effector EspH.

ACKNOLWEDGEMENTS

Foremost, I must express the deepest gratitude to my mentor Dr. Neal Alto for his unfailing support and guidance. His honest and thoughtful advice has helped me design better experiments and think more like a scientist. Additionally, I must thank the members of the Alto Lab from whom I have learned and gained so much. Thanks to fellow graduate students Andrey Selyunin and Robert Orchard for their insight, help, and camaraderie. Most especially, thank you to Sarah Sutton - a wealth of laboratory (and other) wisdom and a perfect lab mate and tutor.

Thanks also to our collaborators, Zhiwei Huang, Lisette Coye, Samuel Miller, and Jijie Chai for their indispensible help in this research. My gratitude also goes to Dr. David Hendrixson and Dr. Nicholas Conrad for serving on my committee and providing aid and moral support during all my time at UT Southwestern.

Finally, I would like to thank my parents, James and Valerie Wallenfang for supporting me at every moment of my life in every way imaginable. I would also like to thank my sister Katie Wallenfang, her fiancé Michael Meyer, and my good friend Matthew Fuller for their advice and moral support.

TABLE OF CONTENTS

LIST OF PUBLICATIONS

Huang, Z., Sutton, S.E., Wallenfang, A.J., Orchard, R.C., Wu, X., Feng, Y., Chan, J., Alto, N.M. (2009) Structural insights into host GTPase isoforms selection by a family of bacterial GEF mimics. Nature Structural and Molecular Biology. In Press.

LIST OF FIGURES

LIST OF DEFINITIONS

Å	Angstroms
A/E	Attaching and Effacing Lesion
BSA	Bovine Serum Albumin
Cdc	Cell Division Cycle Protein
cDNA	Complementary DNA
CFTR	Cystic Fibrosis Transmembrane Conductance Regulator
CNF	Cytotoxic Necrotizing Factor
DNA	Deoxyribonucleic Acid
Dock	Dedicator Of Cytokinesis
DTRL	Deletion Mutation
DTT	Dithiothreitol
Ebp50	Ezrin Binding Protein 50
EDTA	Ethylenediaminetetraacetic Acid
EHEC	Enterohaemorrhagic *E. coli*
ELMO	Engulfment and cell Motility Protein
EPEC	Enteropathogenic *E. coli*

Esp	*E. coli* Secreted Protein
FPLC	Fast Protein Liquid Chromotography
GAP	GTPase Activating Protein
GDF	GDI-displacement factor
GDI	Guanine Nucleotide Dissociation Inhibitor
GDI	Nucleotide Dissociation Inhibitor
GDP	Guanine Diphosphate
GEF	Guanine Nucleotide Exchange Factor
GST	Glutathione S-Transferase
GTP	Guanine Triphosphate
GTPase	Small G-protein
IPTG	isopropyl-beta-D-thiogalactopyranoside
in vitro	Outside the Organism
in vivo	Inside the Organism
LEE	Locus of Enterocyte Effacement
Map	Mitochondrial Associated Protein
Ø	Hydrophobic Amino Acid

PCR	Polymerase Chain Reaction
PDZ	PSD-95, Discs-large, ZO-1
Rac	Ras-related C3 Botulinum Toxin Substrate
Ras	Rat sarcoma
RBD	Rho-binding domains
Rho	Ras Homolog Gene Family Member
SDS-PAGE	Sodium Dodecyl Sulfate Polyacrylamide Gel Electrophoresis
Sif	Salmonella Inducible Filament
SKIP	Ski-interacting protein
Small G-protein	GTPase
Sop	Salmonella Outer Protein
TBS	Tris Buffered Saline
TTSS	type III secretion system
WASP	Wiskott-Aldrich Syndrome Protein
WxxxE	Tryptophan and Glutmate Motif
X	Any Amino Acid
Yop	Yersinia Outer Membrane Protein

CHAPTER 1. INTRODUCTION

Central to the mechanism of *E. coli* pathogenesis is the employment of a specialized type III secretion system (TTSS) (Figure 1) that is encoded on a 35kb chromosomal pathogenicity island termed the locus of enterocyte effacement (LEE) (Figure 2) (McDaniel et al., 1995). The TTSS injects at least 6 proteins, called effectors, directly into host cells (Tir, Map, EspF, EspG, EspH and EspZ). While these 6 effector proteins are encoded on the LEE, recent evidence indicates that several non-LEE encoded effectors also contribute to pathogenesis. These include the experimentally verified cryptic prophage encoded effector EspFu (Campellone et al., 2004; Garmendia et al., 2004) and several Nle effectors (Gruenheid et al., 2004; Kelly et al., 2006; Marches et al., 2005). More recently, Tobe *et al.* identified at least 27 additional type III effectors in a large-scale proteomic analysis of EHEC 0157:H7 secreted proteins (Tobe et al., 2006).

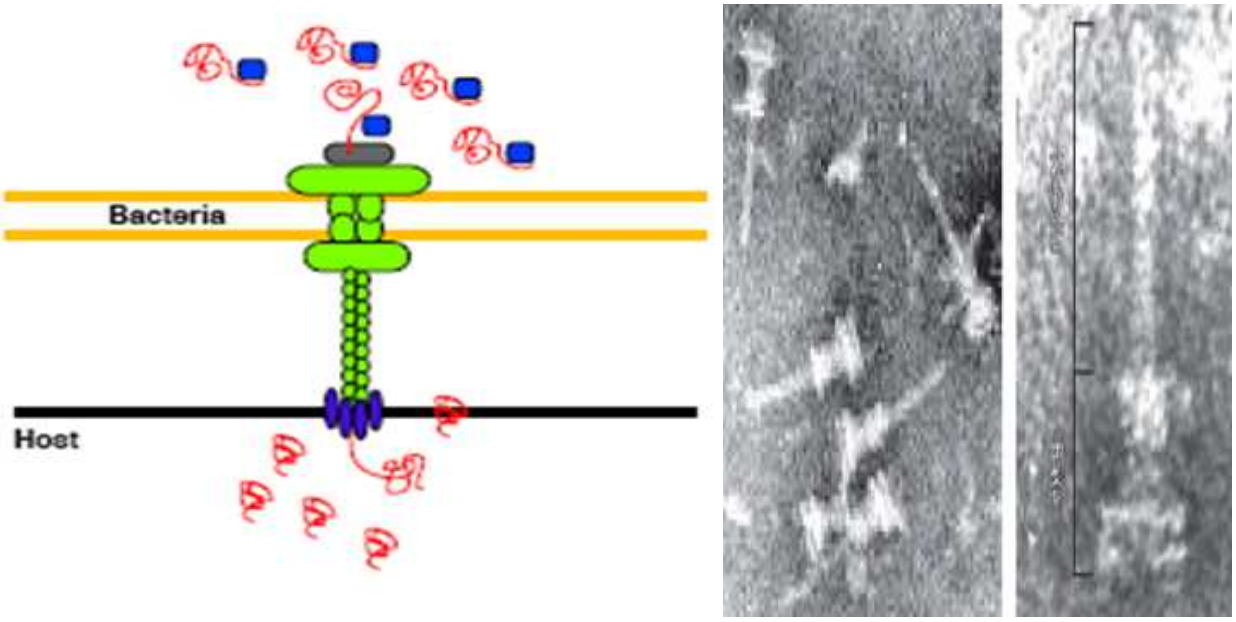

FIGURE 1: The Type Three Secretion System. A cartoon (left) and electron micrograph (right) illustrating the general syringe-like structure of the type three secretion system (TTSS). The cartoon also demonstrates the mechanism of secretion in which effectors arrive at the needle (often shuttled by chaperones), unfold to pass through the needle, and re-fold again on the other side in the host cell cytoplasm.

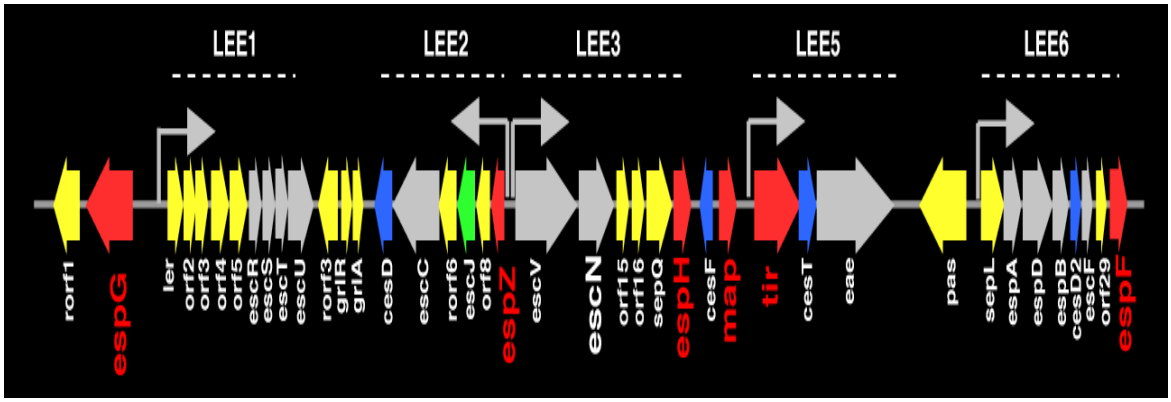

FIGURE 2: The Locus of Enterocyte Effacement. A cartoon schematic of the a 35kb chromosomal pathogenicity island and the several effector and secretion genes it encodes.

In addition to the attaching and effacing *E. coli*, human pathogens such as *Salmonella enterica* and *Shigella flexneri* also rely on a TTSS to cause disease (Galan, 2001; Phalipon and Sansonetti, 2007). Many of the type III effector proteins secreted by *Salmonella* and *Shigella* facilitate host cellular invasion and bacterial persistence within the harsh intracellular environment (Beuzon et al., 2000; Hachani et al., 2008; Ohya et al., 2005; Stein et al., 1996). Our laboratory recently identified a large family of type III effectors found in A/E pathogens as well as *Shigella* and *Salmonella* species (Alto et al., 2006). This family included *E. coli* Map, *Shigella* IpgB1 and IpgB2, as well as *Salmonella* SifA, and SifB. Although these effectors share low overall sequence identity (Map and SifA share less than 13% identity), all of the family members have two invariant amino acids, a tryptophan and glutamic acid found in the WxxxE signature motif. This motif is critical for the so-called "WxxxE" type III effector family members to activate Rho GTPase signaling cascades during bacterial pathogenesis (Alto et al., 2006; Arbeloa et al., 2008).

The X-ray structure of *Salmonella* SifA was recently solved in complex with its human substrate called SKIP (*Ohlson et al. 2008*). This study revealed that SifA has a two-domain architecture; an N-terminal domain mediating the protein interaction with SKIP and the separately folded C-terminal domain that possesses the invariant WxxxE signature motif (*Ohlson et al. 2008*). Remarkably, the WxxxE-containing domain structure of SifA is most similar to SopE, a *Salmonella* type III effector protein with potent guanine-nucleotide exchange activity for Cdc42 (Buchwald et al., 2002; Hardt et al., 1998). However, it is currently unclear if SifA has GEF activity or if any additional WxxxE effectors share a common SopE-like protein fold. Because the primary sequence of SopE and the WxxxE effectors SifA, IpgB1, IpgB2, and Map

are unrelated at the primary amino acid level, we have set out to test if these proteins actually constitute a bacterial superfamily of guanine-nucleotide exchange factors.

Using a combination of yeast genetics, *in vitro* biochemical assays, and bacterial infection studies we demonstrate that the structure of SifA and SopE accurately predicted the cellular activity of two WxxxE effectors, *Shigella* IpgB2 and *E. coli* Map. Importantly, Map has bona fide GEF activity for Cdc42 *in vitro,* and this GEF activity is required for cell surface filopodia induced by Enteropathogenic *E. coli* (EPEC). Finally, our data suggests that the GEF activity of WxxxE effectors may be directly coupled to downstream substrates through their interactions with both GTPase and human scaffolding proteins. These findings reveal a highly sophisticated information transfer mechanism from numerous bacterial pathogens to host actin-cytoskeletal dynamics.

CHAPTER 2. LITERATURE REVIEW

A. Background

Infectious disease has been the leading cause of mortality throughout the history of civilization and remains so even today, particularly in the developing world. The success of pathogens, from viruses to bacteria, has largely been based on their ability to adapt innovative ways of subverting eukaryotic signaling and communication transduction pathways of their host. The objective of usurping these pathways is to circumvent host immune responses and promote the lifecycle of the pathogen. These toxins and effectors demonstrate such a high level of refined adaptation that their study often lends significant insight to the field of cell signaling.

Murine sarcoma viruses were pivotal in the discovery of guanine nucleotide signaling in eukaryotic cells and its roles in human cancer. Ras (Rat sarcoma) genes were first recognized as transduced oncogenes of retroviruses in the 1960s (Harvey, 1964; Kirsten and Mayer, 1969). Ras proteins were then determined to manipulate signaling pathways via a GTPase enzymatic activity. Homology between Ras primary structure and several human proteins led to an explosion of research on small GTPase signaling.

This research has revealed five different subfamilies of Ras GTPase superfamily that, taken as a whole, serve as the signaling gatekeepers of the cell. There are now over 170 known small GTPases and the different subfamilies seem to function in unique cellular roles. The processes of cell division/differentiation, actin cytoskeleton, and nuclear import involve the Ras, Rho, and Ran subfamilies respectively (Takai et al. 2001). Meanwhile, the Arf and Rab subfamily seem to govern intracellular trafficking in all its complexity (Takai et al. 2001). The Ras superfamily also seems to stand at the cross roads of many other signaling networks such as

receptor mediated-, lipid mediated-, and kinase /phosphoatase-, just to name a few (Takai et al., 2001; Colicelli, 2004; Jaffe and Hall, 2005).

B. Small GTpase Signaling

Ras small G-proteins possess numerous characteristics that make them ideal for cellular signaling (Figure 3) (Colicelli, 2004). As the name common GTPase denotes, their primary enzymatic activity is the conversion of bound GTP to GDP via the hydrolysis of the gamma phosphate. When bound to GTP, Ras proteins adopt an activated conformation that allows them to interact with downstream targets. The oscillation between the "off" or GDP-bound form and the "on" or GTP-bound form is facilitated by the action of GTPase activating factors (GAPs) and Guanine Nucleotide Exchange Factors (GEFs) (Figure 4). GAPs accelerate the intrinsic catalytic activity of the GTPase to physiologically relevant levels and lead to the rapid inactivation of a GTPase. GEFs conformationally eject bound GDP from inactivated GTPases allowing the binding of GTP and the activation GTPases and downstream pathways. Lipid modifications also allow GTPase activity to be localized within a eukaryotic cell through association with membranes. Isoprenylation of C-terminal cysteine residues or myristoylation of N-terminal glycine residues are common modifications of the Ras, Rho, and Rab subfamilies and the Arf subfamily respectively. Several other factors are involved in the activity of small G-protein (Figure 3).

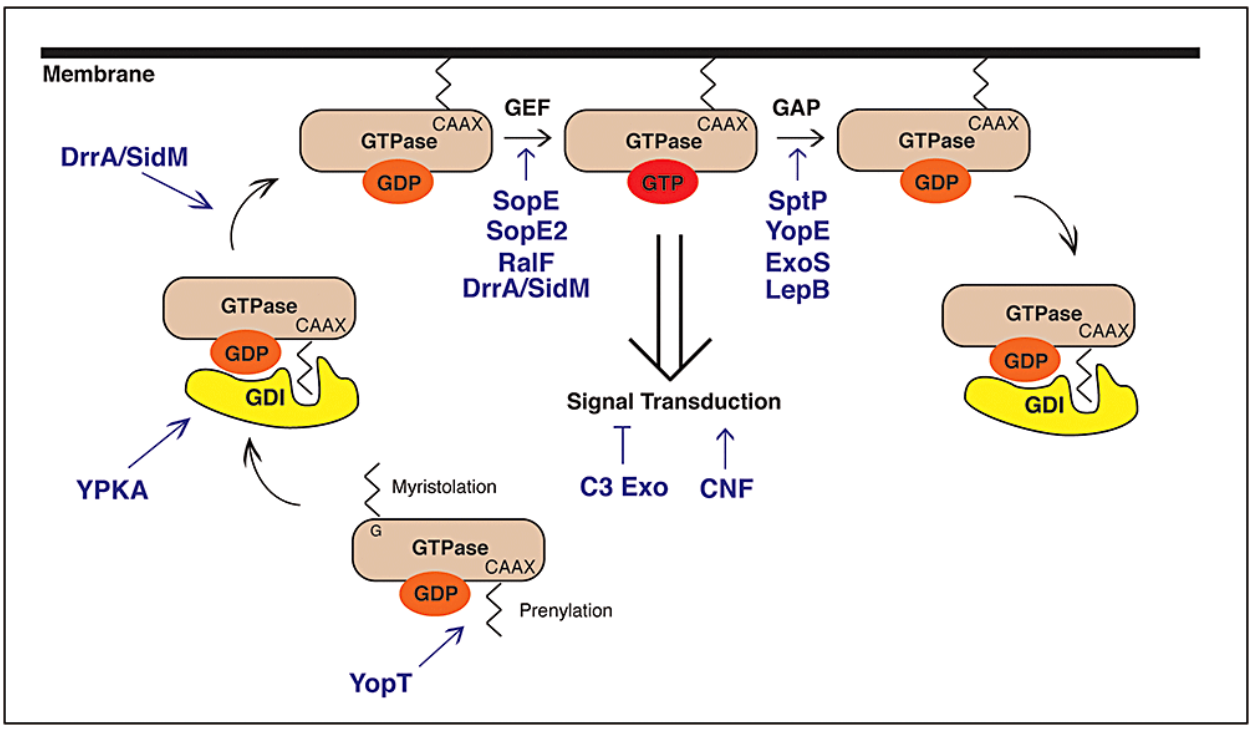

FIGURE 3: Small GTPases Signaling and the Effectors that Target It. Schematic cartoon depicting the signaling cycle of small GTPases and the points of interference by various bacterial effectors.

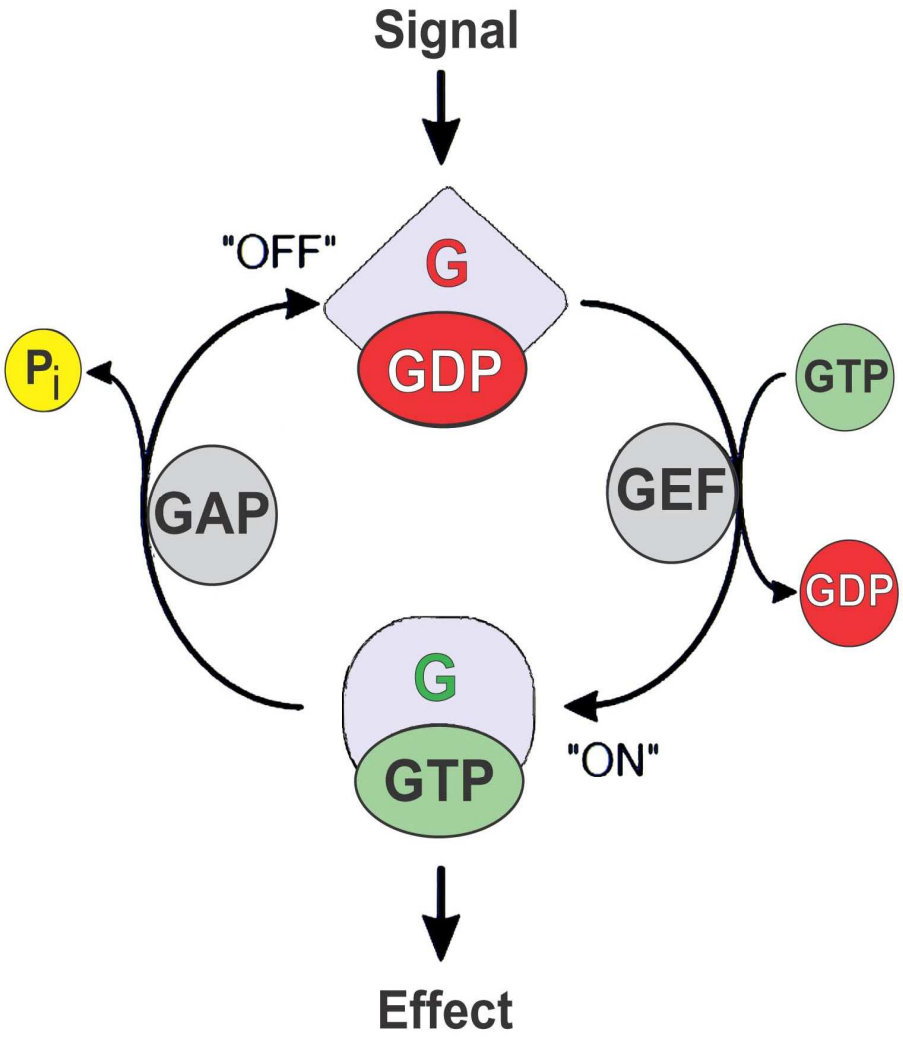

FIGURE 4: The Role of GEFs and GAPs. Schematic cartoon depicting the oscillation of the GTPase molecular circuit via the mediation of GEFs and GAPs.

C. Small GTPases as Targets for Bacterial Effectors

Their switch-like function, preeminence in signaling, and localized activity make GTPases excellent targets for bacterial effectors. For instance, many effectors manipulate the activation state of the GPAse by selective inhibition or activation. It's also been suggested that others may mimic activated GTPase.

Bacterial pathogens have evolved sophisticated methods of activating cell signaling pathways through GTPases. Cytotoxic necrotizing factor (CNF) is a pathogenic *Escherichia coli* toxin that converts Rho to a constitutively active form by deaminating Glutamine 63 of the binding pocket destroying GTP hydrolysis activity and deregulating the actin cytoskeleton (Flatau *et al*. 1997, Schmidt *et al*., 1997). The *Salmonella* TTSS effectors SopE and SopE2 act as GEFs for the GTPases Rac and Cdc42 to facilitate the pathogen's intracellular lifecycle (Hardt *et al*., 1998). Similarly, the Type IV effector RalF acts like a GEF for ARF to promote *Legionella pneumophila* intracellular infection (Nagai *et al*. 2002). Legionella also secretes the hybrid effector DrrA/SidM behaving as both a GEFand a GDF (GDI-displacement factor) to activate Rab1 during maturation of the phagosome (Ingmundson *et al.*, 2007).

Bacterial pathogens have also evolved equally ingenious methods to inhibit GTPase signaling. The *Clostridium botulinum* C3-like exoenzymes irreversibly inhibit Rho by selectively ribosylating Asparagine 41 and thus blocking GTP binding (Aktories and Hall, 1989). Additionally, the activity of GAPs is mimicked by the effectors YopE, SptP, LepB, and ExoS of Yersinia spp., Salmonella spp., Legionella, and Pseudomonas aeruginosa respectively (Fu and Galan, 1999; Pederson *et al*., 1999; Von Pawel-Rammingen *et al*. 2000; Ingmundson *et al*. 2007). Localization is also targeted as a method of inactivation. YopT of *Yersinia* spp.

irreversibly inactivates Rho, Rac, and Cdc42 by cleaving the C-terminal lipids that localize them to membranes (Shao *et al*. 2002). YpkA (YopO), another Yersinia effector, mimics a guanine nucleotide dissociation inhibitor (GDI) by sequestering lipid modified Rho (Prehna *et al*. 2006).

D. The WxxxE family of Type Three Effector Proteins

From the sequencing of several bacterial genomes it is clear that bacteria do not have small GTPases. However, recent studies have nevertheless suggested families of effectors that target the GTPase signaling pathways. One such family was recently determined using bioinformatic searches of TTSS of several pathogenic bacteria (Alto *et al*. 2006). The WxxxE family is defined by the motif of an invariant tryptophan and glutamic acid separated by three variable residues. The discovery of this family lends credence to a previously hypothesized relationship between the effectors of various TTSS pathogens (Brumell *et al.*, 2002). Given the frequent incidence of horizontal gene transfer in bacterial evolution, it is not surprising that such a family might exist between TTSS pathogens, but this family does not contain a high level of homology besides the titular motif.

Upon expression in eukaryotic cells, some WxxxE effectors have been shown to produce phenotypes identical to those seen when over-expressing certain GTPases. The *Shigella* effectors IpgB1 and IpgB2 produce Rac1-characteristic lamellipodia and RhoA-characteristic actin stress fibers (Figure 5) (Ohya *et al*.,2005; Alto *et al*., 2006). The enteropathogenic and enterohaemorrhagic *E. coli* effector Map produces filipodia similar to Cdc42 (Figure 5) (Ohya *et al*.,2005; Alto *et al*., 2006). Mutations in the WxxxE motif destroyed these phenotypes, hinting at shared molecular structure and mechanism in this effector family.

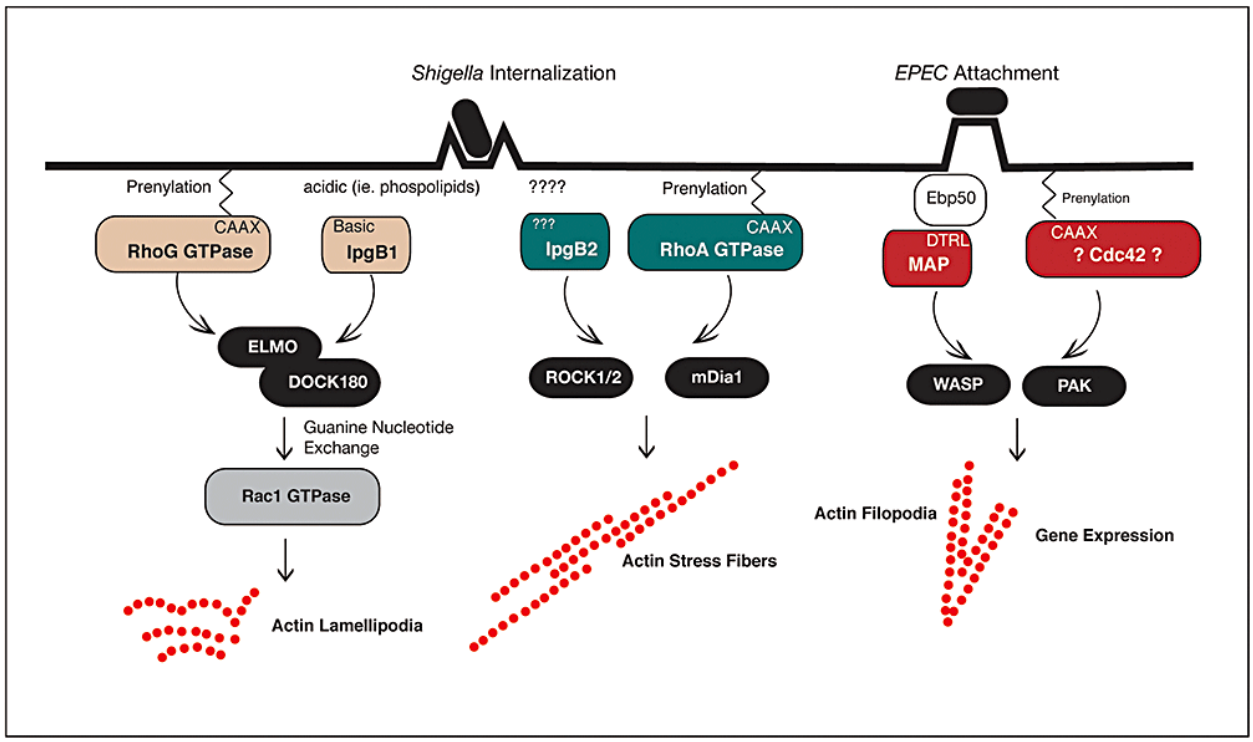

FIGURE 5: WxxxE mimicry of GTPases. Cartoon schematic depicting signaling similarities between the WxxxE effectors IpgB1, IpgB2, and Map and small GTPases RhoG (or Rac1), RhoA, and Cdc42.

Interestingly, the phenotype of IpgB2 seemed to bypass RhoA signaling in mechanism. In the presence of both C3-exoenzyme or YopT, IpgB2 still produced stress fibers (Alto *et al*., 2006). High-throughput yeast genetic screens confirmed this and demonstrated that IpgB2-induced yeast death could be overcome by components of the Rho1p signaling pathway. IpgB2 was also shown to bind the Rho-binding domains (RBD) of three signal pathway members, further suggesting an emulation of RhoA activity. This has led to the hypothesis that the WxxxE family members mimic GTPases (Alto *et al*., 2006).

IpgB1 is necessary for the successful invasion of the host cell by *Shigella flexneri* but, intriguingly, Rac1 has been shown to be activated during infection (Ohya *et al*., 2005). The lamellipodia formation seen in both IpgB1 expression and Rac1 over-expression (Hall, 1998) appears to be responsible for Shigella uptake into non-phagocytic cells. IpgB1 has subsequently been shown to bind to engulfment and cell motility (ELMO) protein (Handa *et al*. 2007), which sits at the crossroads of signaling pathways of both Rac1 and RhoG in the formation of lamellipodia and apoptotic cell uptake (Katoh and Negishi, 2003). The mimicking hypothesis was further supported by experiments demonstrating IpgB1 imitation of RhoG.

Map is encoded by the LEE pathogenicity island in all attaching and effacing (A/E) pathogens (EPEC, EHEC, and *Citrobactor rodentium*). A/E pathogens are named for the lesions they produce via the strong adherence to the apical surface of intestinal epithelial cells, effacement of microvilli, and undermining of the epithelial barrier (Moon *et al*. 1983). Orginally named for its localization to mitochondria during infection (mitochondrial associated protein) (Kenny and Jepson, 2000), Map also seems to be responsible for filipodia formation during early infection (Kenny *et al*. 2002). Like IpgB1 and Rac1, while Map appears to activate Cdc42 during infection, neither Cdc42 nor its downstream target WASP appeared to be necessary for

the filipodia phenotype (Lommel *et al*., 2001; Snapper *et al*., 2001). Thus Map also appeared to fit into the WxxxE mimic narrative.

Like GTPases, several members of the WxxxE family have evolved motifs that allow specific localization within the host cell. Map, for instance, contains a motif that recognizes and binds the PDZ (PSD-95, Discs-large, ZO-1) domains of signaling proteins (Alto *et al*., 2006; Simpson *et al.*, 2006). PDZ domains promote the protein-protein interactions between C-termini necessary for assembling scaffolding arrangements during cellular signaling (Pawson and Scott, 1997). Such scaffolds are pivotal in many different cellular processes and are a common target during infectious disease (Obenauer *et al*., 2006). Two different classes of C-terminal motifs are recognized by PDZ domains. Class 1 presents a sequence of [X-(T/S)-X-$Ø_{COOH}$] and Class 2 presents a sequence of [X-Ø-X $Ø_{COOH}$] in which X is any residue and Ø is a hydrophobic residue (Songyang *et al*., 1997). Map has a class 1 PDZ ligand identical to the eukaryotic protein CFTR (Alto *et al*. 2006), and like CFTR binds the membrane enriched adapter (Bretscher *et al*., 2000) Ezrin binding protein 50 (Ebp50) via PDZ protein-protein interaction (Short *et al*., 1998; Alto et al., 2006; Simpson et al., 2006). Thus it is possible that the PDZ sequence allows Map to be localized to the apical cellular membrane.

Other WxxxE family members possess similar targeting motifs. A 105 residue N-terminal targeting sequence localizes IpgB1 to the lamellipodial protrusions during infection allowing activation of the Elmo/Dock180 complex (Handa *et al*, 2007). SifA has a C-terminal motif that appears to mimic the CaaX box that gets lipid modified in many GTPases and this motif is essential for SifA localization to Salmonella inducible filaments during infection (Boucrot et al., 2003). Thus, the WxxxE family demonstrates to have a diverse array of independently evolved mechanisms for directing strategic placement in the host cell.

CHAPTER 3. RESULTS

A. Sequence Analysis of the WxxxE effectors based on the X-ray structure of SifA and its structural homology to *Salmonella* SopE

We have recently determined the first structure of a WxxxE motif containing protein to 2.6Å resolution (*Ohlson et al., 2008)*. The atomic model of *Salmonella* SifA revealed that the region of homology surrounding the WxxxE motif (residues 178-327) is composed of six alpha helices that form a V-shaped structure (Figure 6). The WxxxE-containing domain of SifA is most similar in structure to SopE (Figure 7) (*Ohlson et al. 2008*), a *Salmonella* type III effector protein with potent GEF activity for Cdc42 (Buchwald et al., 2002; Hardt et al., 1998). Despite the convergent tertiary structures of these two *Salmonella* effectors, their primary structures share no homology. Moreover, no GEF activity has been observed for SifA or any WxxxE effector.

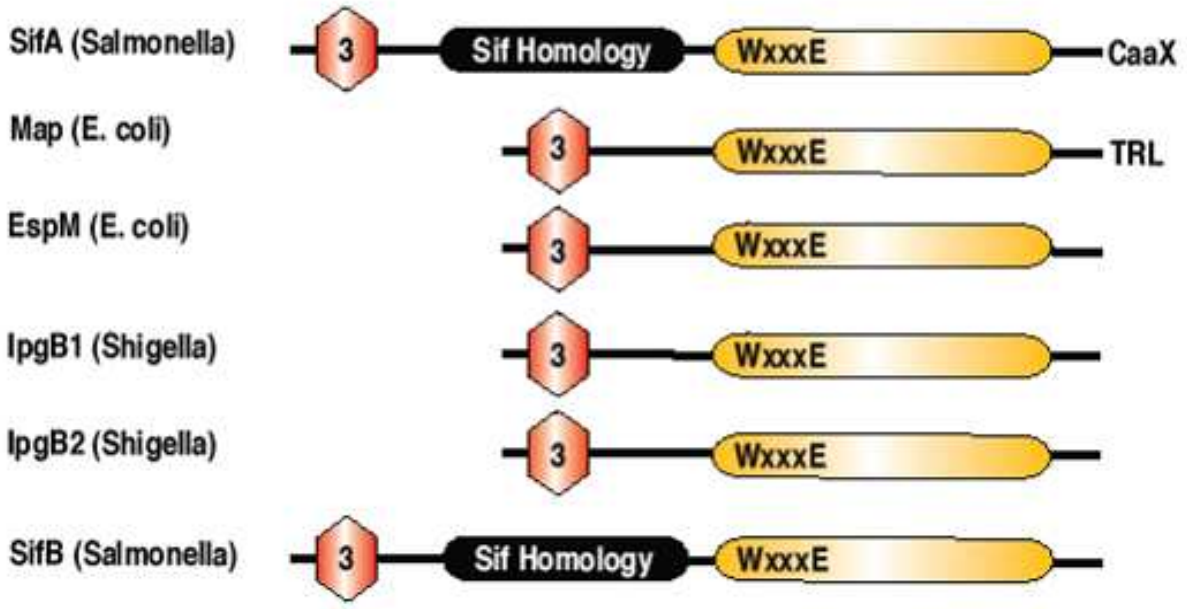

FIGURE 6: Comparison of Several WxxxE Family Members. Domain architecture of WxxxE proteins shown TTSS signal (red), Sif homology domain (black) and the WxxxE homology domain (orange).

FIGURE 7: Comparison of SifA and SopE Tertiary Structure. Overall structure of SifA 178-327 compared to SopE.

WxxxE Domain Fold of SifA

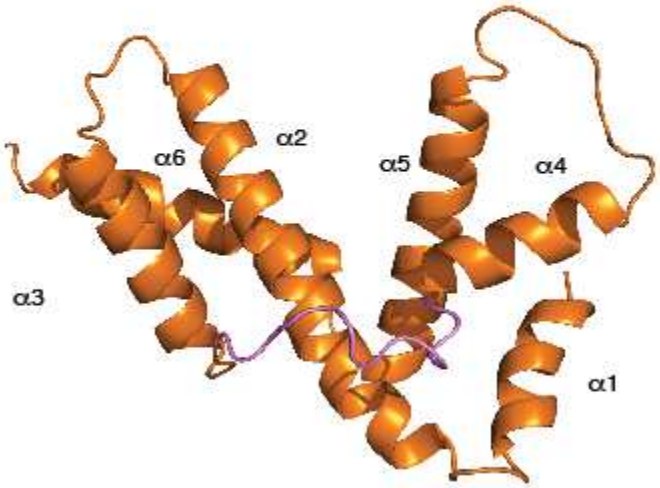

GEF Domain Fold of SopE

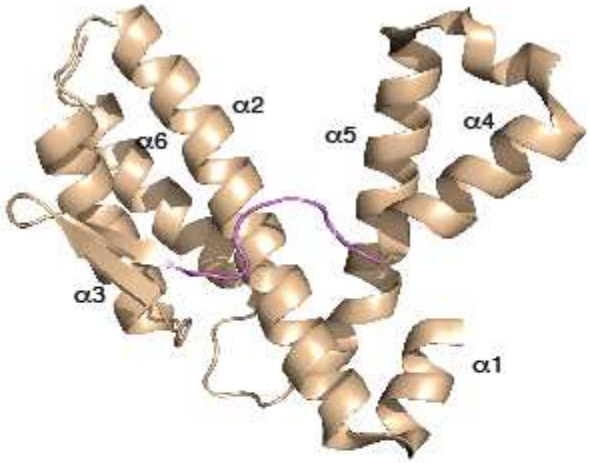

Buchwald et al. identified key residues of SopE that make direct contact with host Cdc42 (Buchwald et al., 2002). Several of these contact residues are involved in the nucleotide exchange reaction catalyzed by SopE. Therefore, the SopE*Cdc42 contact sites were directly mapped onto the surface structure of SifA (Figure 8). In addition, the amino acid sequences encompassing the six-helical bundle of SopE and SifA were aligned to several WxxxE effectors by ClustalW algorithm (Figure 9). This allowed us to extrapolate the SopE*Cdc42 contact sites mapped to SifA directly to the sequences of SifB, Map, EspM1, IpgB1, and IpgB2 (Figure 9, purple residues).

FIGURE 8: Analogous motifs of SifA and SopE. Sequence analysis of the WxxxE effector family. A surface projection of SifA 178-327. The SopE*Cdc42 contact positions mapped onto the surface of SifA are labeled (purple) and a surface exposed α2 helix residue that is not functional is shown (red). Performed by Robert Orchard.

SifA Surface Structure

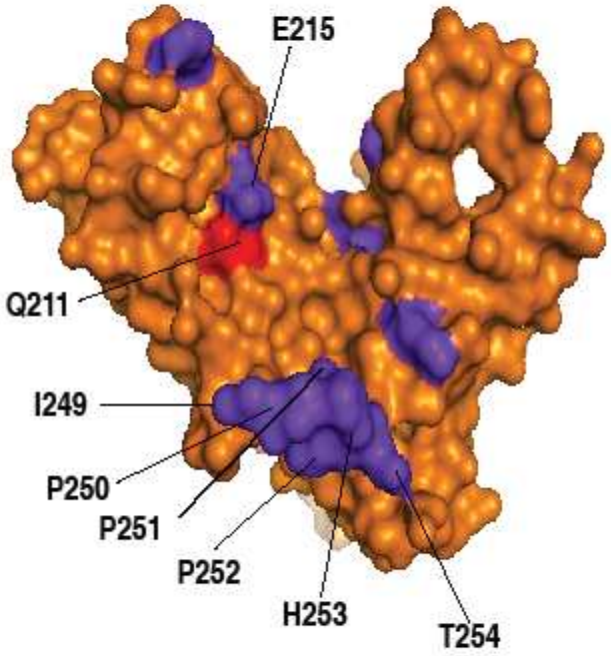

FIGURE 9: ClustalW sequence alignment of the WxxxE effectors compared to SopE and SifA. Gene name and bacterial species are indicated. The six alpha helices comprising SifA residues 178-327 are labeled a1-a6 (orange) as the convention of SopE GEF structure previously reported (green) (Buchwald et al., 2002). The SopE contact sites with Cdc42 and the corresponding contract sites in type III effectors are shown (purple). The invariant WxxxE motif, the SopE D124 contact residue, and the AQSSI motif are each boxed. The non-functional surface exposed residue is highlighted in red. Arrows indicate the residues mutated in IpgB2 for Figure 1D and 1E. Performed by Neal Alto.

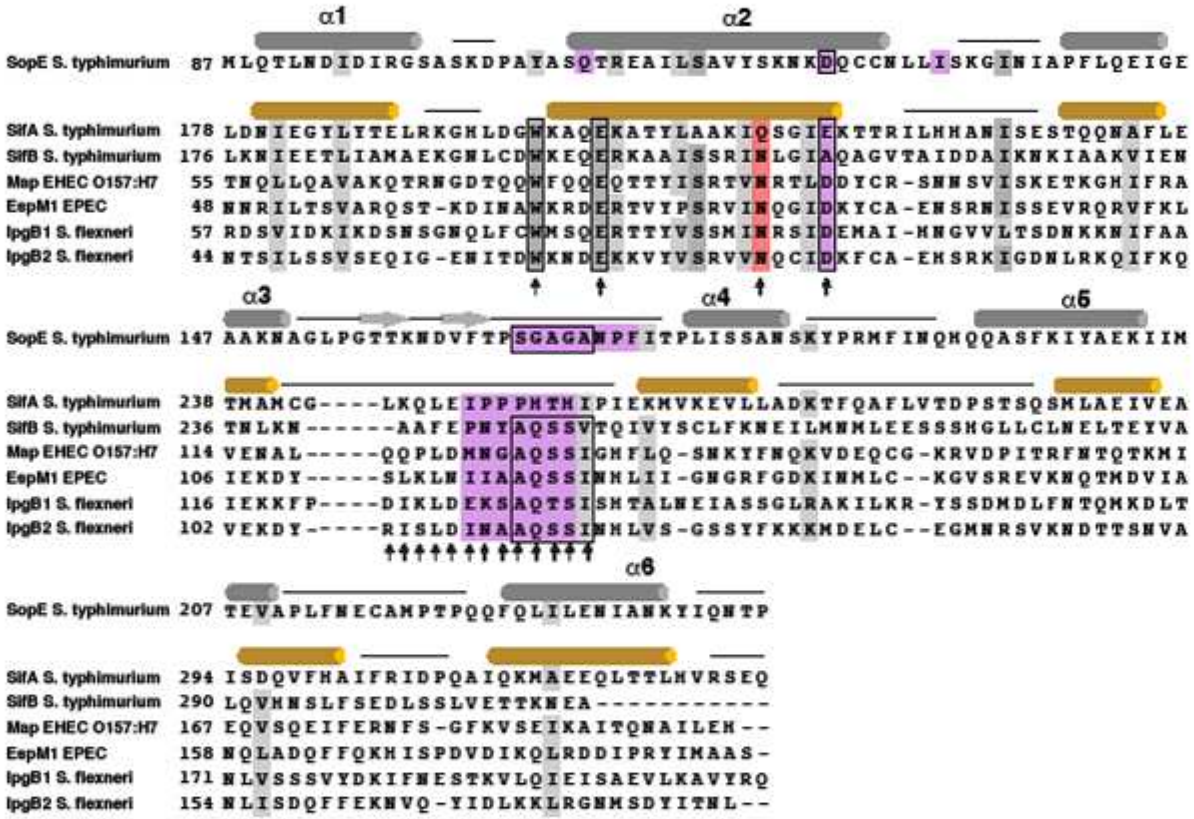
α1
α2
SopE S. typhimurium 87 MLQTLNDIDIRGSASKDPAYASQTREAILSAVYSKNKDQCCNLLISKGINIAPFLQEIGE
SifA S. typhimurium 178 LDNIEGYLITELRKGHLDGWKAQEKATYLAAKIQSGIEKTTRILHHANISESTQQNAFLE
SifB S. typhimurium 176 LKNIEETLIAMAEKGNLCDWKEQERKAAISSRINLGIAQAGVTAIDDAIKNKIAAKVIEN
Map EHEC O157:H7 55 TNQLLQAVAKQTRNGDTQQWFQQEQTTYISRTVNRTLDDYCR-SNNSVISKETKGHIFRA
EspM1 EPEC 48 NNRILTSVARQST-KDINAWKRDERTVYPSRVINQGIDKYCA-ENSRNISSEVRQRVFKL
IpgB1 S. flexneri 57 RDSVIDKIKDSNSGNQLFCWMSQERTTYVSSMINRSIDEMAI-HNGVVLTSDNKKNIFAA
IpgB2 S. flexneri 44 NTSILSSVSEQIG-ENITDWKNDEKKVYVSRVVNQCIDKFCA-ENSRKIGDNLRKQIFKQ
α3
α4
α5
SopE S. typhimurium 147 AAKNAGLPGTTKNDVFTPSGAGANPFITPLISSANSKYPRMFINQHQQASFKIYAEKIIM
SifA S. typhimurium 238 TMAMCG----LKQLEIPPPMTHIPIEKMVKEVLLADKTFQAFLVTDPSTSQSMLAEIVEA
SifB S. typhimurium 236 TNLKN------AAFEPNYAQSSVTQIVYSCLFKNEILMNMLEESSSHGLLCLNELTEYVA
Map EHEC O157:H7 114 VENAL-----QQPLDMNGAQSSIGHFLQ-SNKYFNQKVDEQCG-KRVDPITRFNTQTKMI
EspM1 EPEC 106 IEKDY-----SLKLNIIAAQSSINNLII-GNGRFGDKINMLC--KGVSREVKNQTMDVIA
IpgB1 S. flexneri 116 IEKKFP----DIKLDEKSAQTSISHTALNEIASSGLRAKILKR-YSSDMDLFNTQMKDLT
IpgB2 S. flexneri 102 VEKDY-----RISLDINAAQSSINNHLVS-GSSYFKKKMDELC--EGMNRSVKNDTTSNVA
α6
SopE S. typhimurium 207 TEVAPLFNECAMPTPQQFQLILENIANKYIQNTP
SifA S. typhimurium 294 ISDQVFHAIFRIDPQAIQKMAEEQLTTLHVRSEQ
SifB S. typhimurium 290 LQVHNSLFSEDLSSLVETTKNEA----------
Map EHEC O157:H7 167 EQVSQEIFERNFS-GFKVSEIKAITQNAILEH--
EspM1 EPEC 158 NQLADQFFQKHISPDVDIKQLRDDIPRYIMAAS-
IpgB1 S. flexneri 171 NLVSSSVYDKIFNESTKVLQIEISAEVLKAVYRQ
IpgB2 S. flexneri 154 NLISDQFFEKNVQ-YIDLKKLRGNMSDYITNL--

The complementary views of protein structure and sequence alignment were used as a reference template in subsequent structure/function studies on the WxxxE effector *Shigella* IpgB2. IpgB2 activates the RhoA GTPase signaling pathway in human cells and the orthologous Rho1p GTPase signaling pathway in yeast (Figure 10) (Alto et al., 2006). In fact, hyperactivation of yeast Rho1p induced a severe growth arrest phenotype in IpgB2 expressing cells (Figure 10) (Alto et al., 2006). Therefore, this simple life and death assay was used as an unambiguous readout of IpgB2 function in yeast.

FIGURE 10: Yeast Expression Protocol. Schematic of yeast expression protocol and the Rho1p pathway that was previously shown to be activated by IpgB2 (Alto et al., 2006).

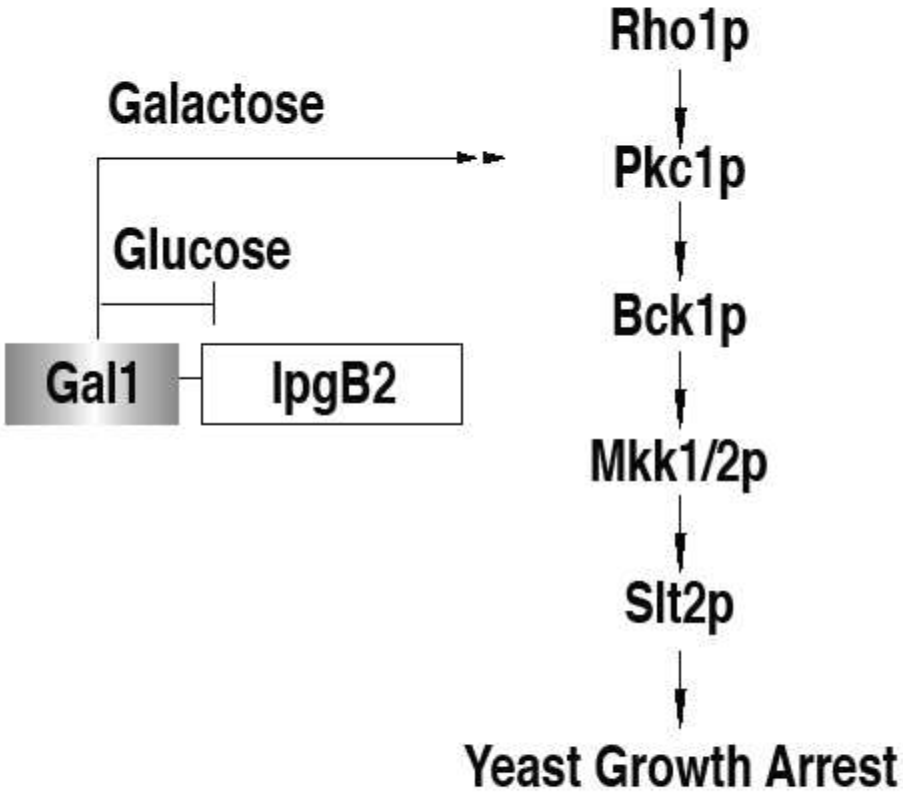
Galactose
Glucose
Gal1
IpgB2
Rho1p
Pkc1p
Bck1p
Mkk1/2p
Slt2p
Yeast Growth Arrest

The GEF catalytic mechanism of SopE relies on the loop residues SGAGA found between α3 and α4 (Figure 11, purple) (Buchwald et al., 2002). These residues are inserted between switch I and switch II to disrupt the nucleotide-binding pocket and facilitates guanine-nucleotide exchange. We have detailed the equivalent surface exposed residues of SifA and mapped these residues to the sequence of IpgB2 in Figure 9 (arrows). Importantly, this alignment suggests that a fourteen-residue sequence may confer the α3-α4 loop region of most WxxxE effectors including IpgB2. First, we deleted the highly conserved AQSSI sequence of IpgB2 that aligned to the SGAGA sequence of SopE. IpgB2ΔAQSSI was non-functional as yeast grew normally upon selective expression of this gene (Figure 12). To further define the putative loop region, we individually mutated all 14 residues that included the AQSSI sequence. As shown in Figure 11, mutations between 107-111 had no effect on IpgB2 activity whereas residues I112, S117, and I119 conferred a loss of function phenotype. Interestingly, I112 of IpgB2 is in the equivalent position as I249 of SifA, a surface exposed loop residue (see Figure 8) that is predicted to make contact with GTPases (*Ohlson et al. 2008*). Moreover, S117 and I119 are found in the conserved AQSSI motif (see Figure 9) further supporting the notion that this is an important region of functionality.

FIGURE 11: Comparison of SifA and SopE catalytic loop. Structural view of the GEF catalytic loop of SifA and the corresponding loop in SopE (purple). The residues W197 and E201 of the WxxxE motif (cyan) are analogous to residues Y106 and T110 of SopE (cyan) that stabilize the base of the GEF loop.

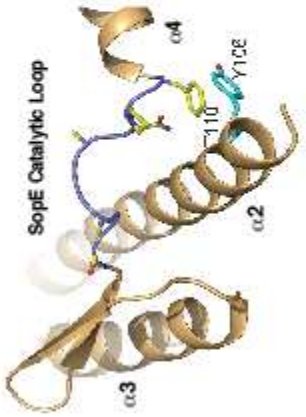
SopE Catalytic Loop
α4
α2
α3

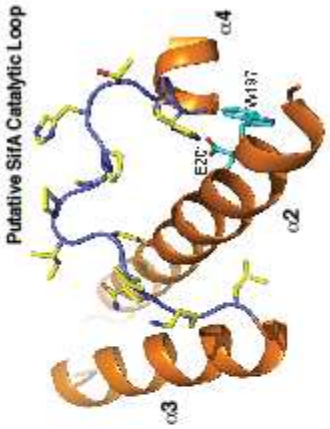
Putative SifA Catalytic Loop
α4
α2
α3

FIGURE 12: Yeast Growth Assay I. Yeast growth assay of IpgB2 mutants patched to galactose medium (IpgB2 expression) or control glucose medium (no expression). IpgB2 mutants are indicated by each reference grid. Performed by Neal Alto and Sarah Sutton.

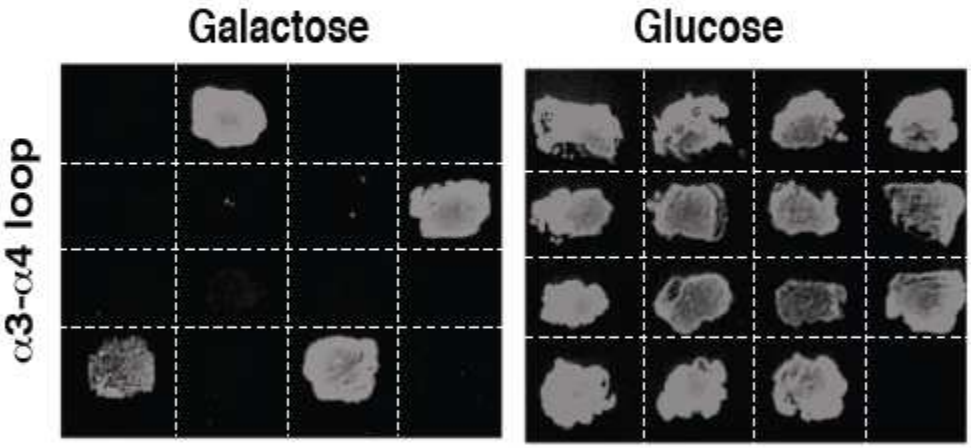

Wt	Δ AQSSI	R107K	I108A
S109A	L110A	D111N	I112A
N113A	A114S	A115S	Q116A
S117A	S118A	I119A	

Besides the SGAGA sequence in the SopE catalytic loop, the acidic D124 of SopE makes extensive contacts with Switch I region of Cdc42 (Buchwald et al., 2002) (Figure 9, purple). This charged residue is highly conserved in human Dbl-like GEFs (Rossman et al., 2002; Worthylake et al., 2000) and mutations in D124 inactivates SopE (Schlumberger et al., 2003). We noted that an equivalent acidic residue is found on the surface of α2 helix of SifA (E215) and this negative charge is conserved among WxxxE effectors (Figure 9). Mutation in D80 of IpgB2 (equivalent to SopE D124) abolished its ability to kill yeast and presumably to interact with Rho1p (Figure 13). This was not simply due to mutating any surface residue on α2 since mutation of IpgB2 N76 conferred a growth defect in yeast. Consistent with our previous report W62A (not shown) and E66A (Figure 1E) mutations abolished yeast toxicity (Alto et al., 2006) further suggesting that α2 helix is a key structural element of IpgB2 function. All together, these data support the notion that IpgB2 adopts a helical V-shaped structure similar to SifA and that WxxxE effectors may activate GTPase signaling pathways in an analogous fashion as SopE.

FIGURE 13: Yeast Growth Assay II. Yeast growth assay of IpgB2 mutants patched to galactose medium (IpgB2 expression) or control glucose medium (no expression). IpgB2 mutants are indicated by each reference grid. Performed by Neal Alto and Sarah Sutton.

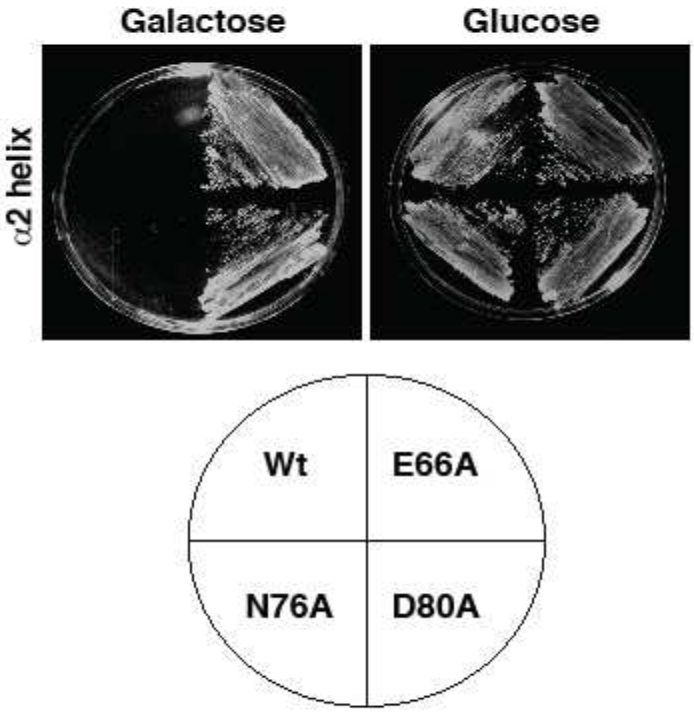
Galactose
Glucose
α2 helix
Wt
E66A
N76A
D80A

B. Screening WxxxE effectors for GEF activity.

To determine if any of the WxxxE effectors could bind Rho proteins *in vitro*, we took advantage of the fact that GEF proteins form stable complexes with cognate GTPases in their nucleotide free form. Nucleotide free GST-tagged RhoA, Cdc42 and Rac1 were incubated with purified Maltose Basic Protein (MBP) tagged IpgB2, Map, and SifA, three WxxxE effectors from *Shigella, E. coli, Salmonella* respectively. Protein complexes were isolated by glutathione sepharose pulldown (GST-pulldown), washed several times with binding buffer and run on SDS-PAGE. As shown in Figure 14, EHEC O157:H7 Map formed a stable complex with Cdc42 at an apparent 1:1 stoichiometry. We observed a low level of binding of SifA to Cdc42, however none of the other small G-proteins associated with WxxxE effectors under these specific experimental conditions.

FIGURE 14: Map Interacts with Cdc42. GST pull-down of 10ug nucleotide free RhoA, Cdc42 and Rac1 incubated with 20ug of MBP control, MBP-IpgB2, MBP-Map, and MBP-SifA. SDS-PAGE gels stained with Coomassie Brilliant Blue were used to detect protein interactions. Map bound Cdc42 with an apparent 1:1 stoichiometry. Performed by Sarah Sutton.

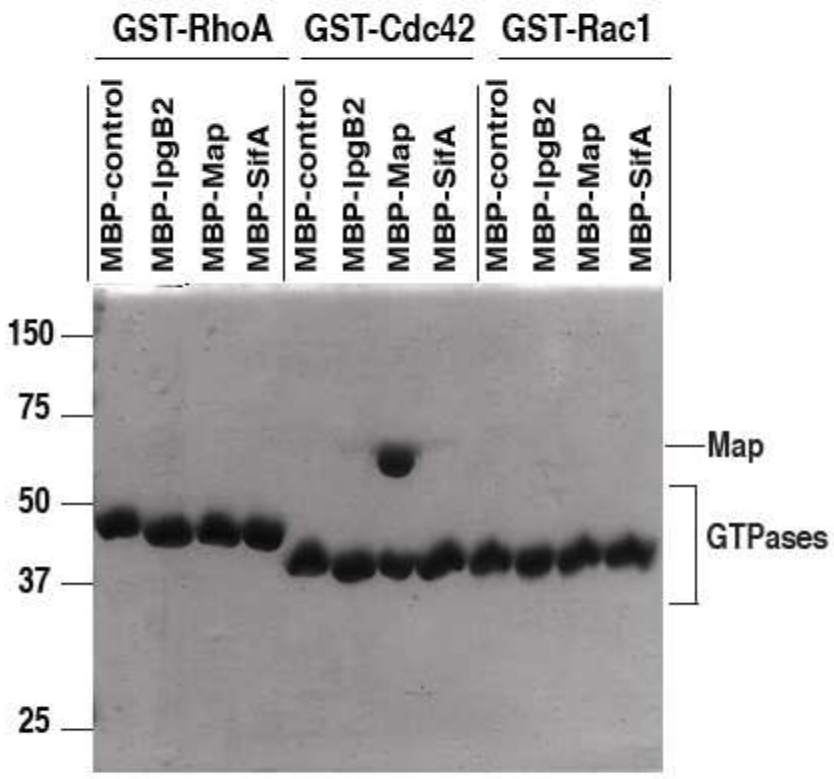
GST-RhoA
GST-Cdc42
GST-Rac1
MBP-control
MBP-IpgB2
MBP-Map
MBP-SifA
MBP-control
MBP-IpgB2
MBP-Map
MBP-SifA
MBP-control
MBP-IpgB2
MBP-Map
MBP-SifA
150
75
50
37
25
Map
GTPases

Next, we tested if any WxxxE effectors catalyzed guanine-nucleotide exchange on Rho GTPases. To initiate the nucleotide exchange reaction, radiolabelled $GTP\gamma S^{35}$ and 1μM WxxxE effectors were added to GDP loaded RhoA, Cdc42 or Rac1. The reactions were stopped after 10 minutes and the newly formed $GTP\gamma S^{35}$ GTPases were monitored by filter binding assays. As shown in Figure 15, Map induced a robust guanine-nucleotide exchange on Cdc42. We observed a basal GEF activity with SifA (Figure 15), however this activity was significantly lower than the GEF activity of Map. Surprisingly, neither *Shigella* IpgB2 (Figure 2B) nor the *Salmonella* WxxxE effector SifB (data not shown) had any GEF activity against these GTPases. In addition, it was also surprising that Map bound Cdc42 but not Rac1, a closely related GTPase that is often associated with Cdc42 GEFs. To define the GTPase selectivity of Map, fifteen Rho-family members were screened for binding interactions under nucleotide free conditions. As shown in Figure 16, Map exclusively bound Cdc42 *in vitro* and did not bind to any other GTPase tested.

FIGURE 15: Map Activates Cdc42. Guanine-nucleotide exchange assays were performed on GDP loaded GTPases (1μM). Reactions were performed by adding each WxxxE effector or MBP control proteins (1μM) to Rho, Cdc42, or Rac1 with radiolabelled GTP□S^{35}. Nucleotide exchange was conducted for 10 minutes and the incorporation of new GTP□S^{35} into the GTPase was monitored by filter binding assay and scintillation counting the S^{35} radioisotope (cpm). Results are representative of three independent experiments. Performed by Robert Orchard.

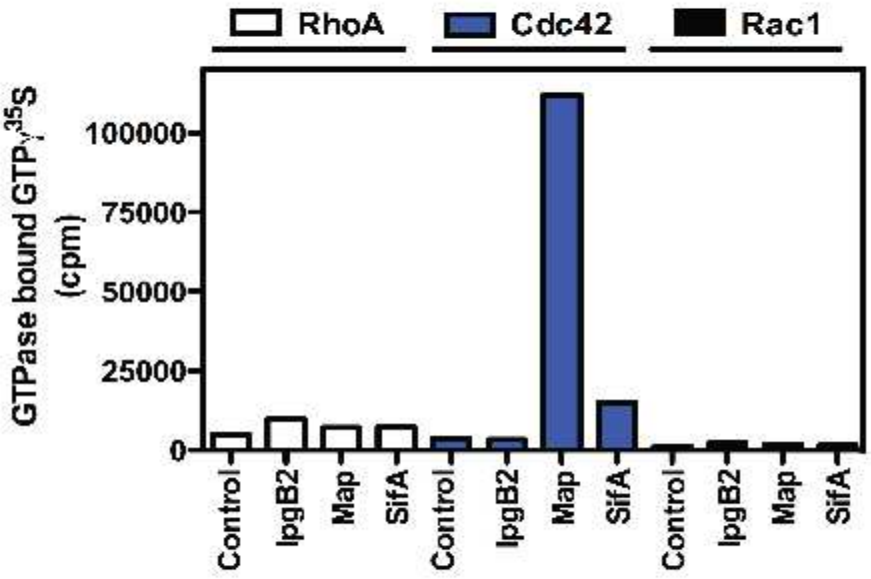
RhoA
Cdc42
Rac1
GTPase bound GTPγ35S (cpm)
100000
75000
50000
25000
0
Control
IpgB2
Map
SifA
Control
IpgB2
Map
SifA
Control
IpgB2
Map
SifA

FIGURE 16: Map is Specific for Cdc42. GST pull-down of 10ug nucleotide free GST-GTPases incubated with 20ug of MBP-Map. SDS-PAGE gels stained with Coomassie Brilliant Blue were used to detect protein interactions. Map bound Cdc42 with an apparent 1:1 stoichiometry but did not interact with any other GTPase tested.

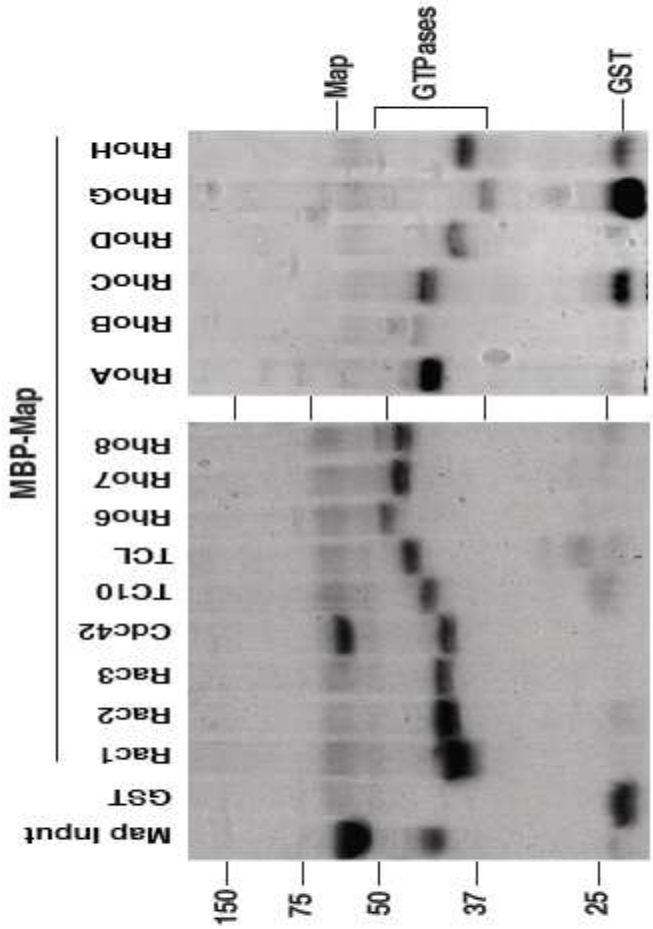
Map
GTPases
GST
MBP-Map
RhoH
RhoG
RhoD
RhoC
RhoB
RhoA
Rho8
Rho7
Rho6
TCL
TC10
Cdc42
Rac3
Rac2
Rac1
GST
Map input
150
75
50
37
25

A detailed kinetic analysis of the GDP/GTP exchange reaction further indicated that Map is a potent Cdc42 GEF *in vitro*. Map induced the release of [^{3}H]-GDP with a half-time of 78 seconds (Figure 17, blue circles) compared to MBP control protein (Figure 17, white squares). These values are within the experimental error of [^{35}S]-GTPgS nucleotide-exchange rate on Cdc42 that we determined for Map (Figure 18, $t_{1/2}$= 43 sec.). In addition, a saturation-binding curve generated from the Map GEF activity assays were used to estimate its apparent Cdc42 dissociation constant (K_D) to the sub micro-molar range (~236nM, data not shown). Importantly, the guanine-nucleotide exchange activity of Map is similar to the previously reported Cdc42 GEF activity of SopE (Hardt et al., 1998) and human *dbl (Hart et al., 1991)* under similar experimental conditions. Therefore, our findings confirm that Map is a bona fide GEF *in vitro*, a postulate that strongly confirms a structural analogy between WxxxE effectors and SopE.

FIGURE 17: Map is a Potent GEF for Cdc42 I. Time course of Cdc42 guanine nucleotide exchange catalyzed by 1μM Map (blue circles) or MBP control protein (white box). [^{3}H]-GDP release assays (**D**) and GTP□S^{35} binding assays (**E**) were performed on 1μM Cdc42. Half-time measurements were derived from the curves fit to these data by non-linear regression. Results are representative of three independent experiments.

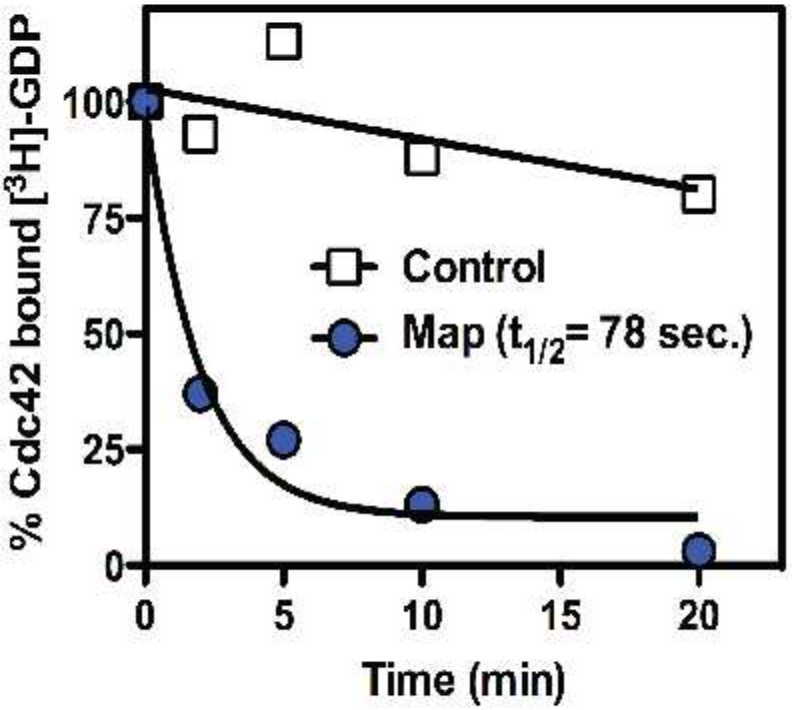
% Cdc42 bound [3H]-GDP
100
75
50
25
0
0
5
10
15
20
Time (min)
Control
Map (t1/2= 78 sec.)

FIGURE 18: Map is a Potent GEF for Cdc42 II. Time course of Cdc42 guanine nucleotide exchange catalyzed by 1μM Map (blue circles) or MBP control protein (white box). [^{3}H]-GDP release assays were performed on 1μM Cdc42. Half-time measurements were derived from the curves fit to these data by non-linear regression. Results are representative of three independent experiments.

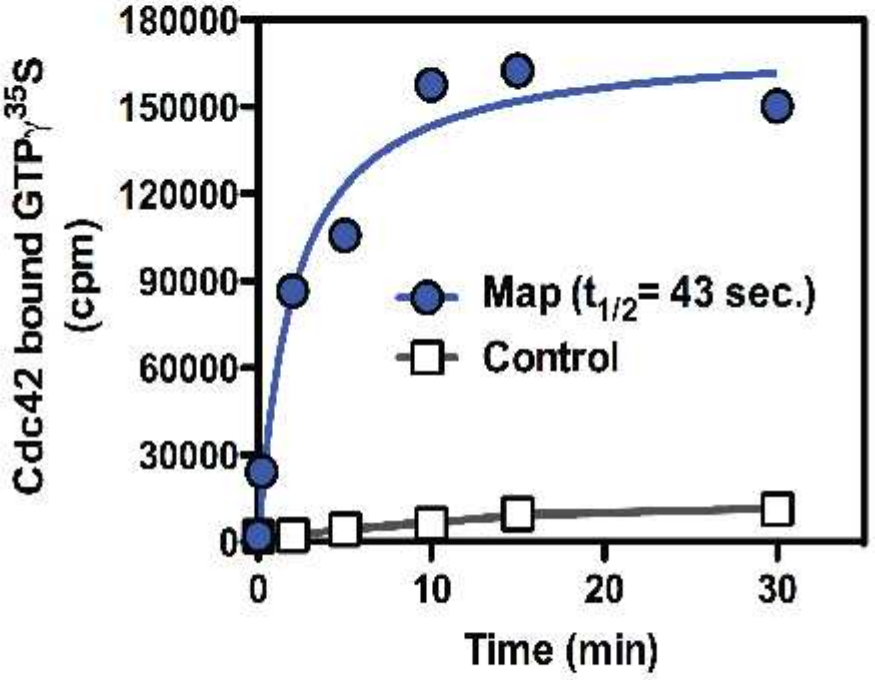
180000
150000
120000
90000
60000
30000
0
Cdc42 bound GTPγ35S (cpm)
Map (t1/2= 43 sec.)
Control
0
10
20
30
Time (min)

C. Structure/functional analysis of Map as a SopE-like GEF.

Map and SopE have potent GEF activity for Cdc42. However these effectors share no clear sequence homology to suggest that they function through common molecular mechanism (see Figure 9). However, the SopE GEF-catalytic loop is similarly structured to the α3-α4 loop region of SifA, a protein that has been suggested to be related to Map (Figure 11). Therefore, we performed experiments that would either support or invalidate the idea that Map and SopE function through a similar GEF catalytic mechanism.

Our previous data suggested the possibility that conserved residues surrounding the AQSSI sequence of IpgB2 may perform a similar function as the SGAGA catalytic loop of SopE (Figure 11). We found that wild-type Map but not a deletion mutant MapΔAQSSI mutant formed a stable protein complex with nucleotide free GST-Cdc42 *in vitro* (Figure 19). Likewise, wild-type Map induced the release of GDP from Cdc42 (Figure 20) and promoted GDP/GTP exchange (Figure 21) whereas MapΔAQSSI had significantly attenuated GEF activity in these assays (Figure 20 and 21). Without a co-complex structure of Map and Cdc42 we cannot definitively conclude that the AQSSI residues are functionally equivalent to the SGAGA motif of SopE. However, these data do support the existence of a α3-α4 loop region that catalytically activates Cdc42.

FIGURE 19: WxxxE Motif and Putative Catalytic Loop are Necessary for Map GEF Activity I. [^{3}H]-GDP release assays of 1μM Cdc42 and 1μM of MBP-Map and the indicated mutants. The average of four experiments is shown (SEM).

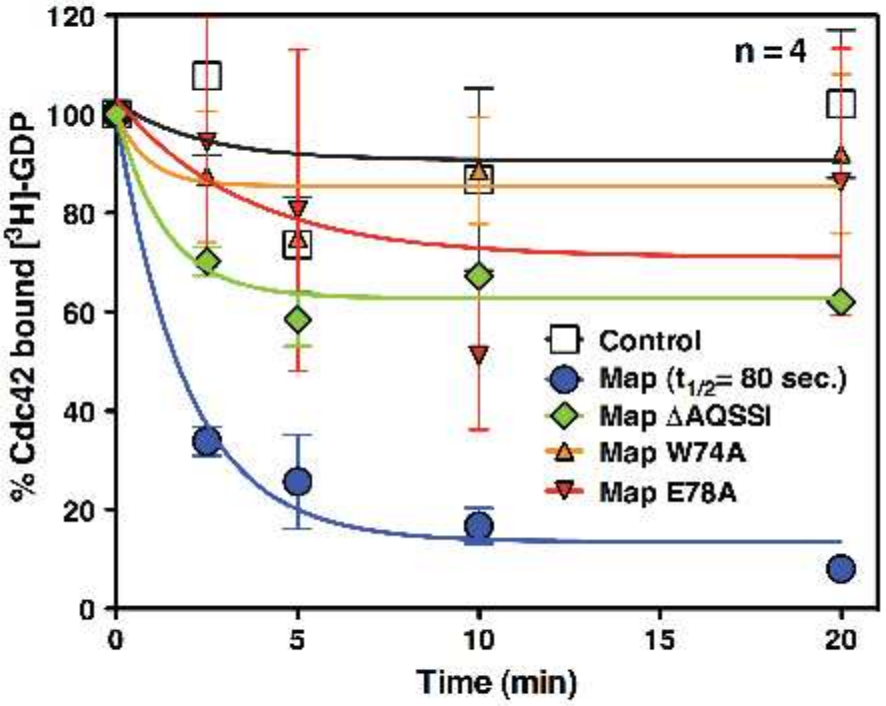
n = 4
% Cdc42 bound [3H]-GDP
Time (min)
Control
Map (t1/2= 80 sec.)
Map ΔAQSSI
Map W74A
Map E78A
0
20
40
60
80
100
120
0
5
10
15
20

FIGURE 20: WxxxE Motif and Putative Catalytic Loop are Necessary for Map GEF Activity II. Cdc42 guanine nucleotide exchange of GTP□S^{35} catalyzed by 1μM of the proteins indicated. Experiments were performed as in Figure 2B.

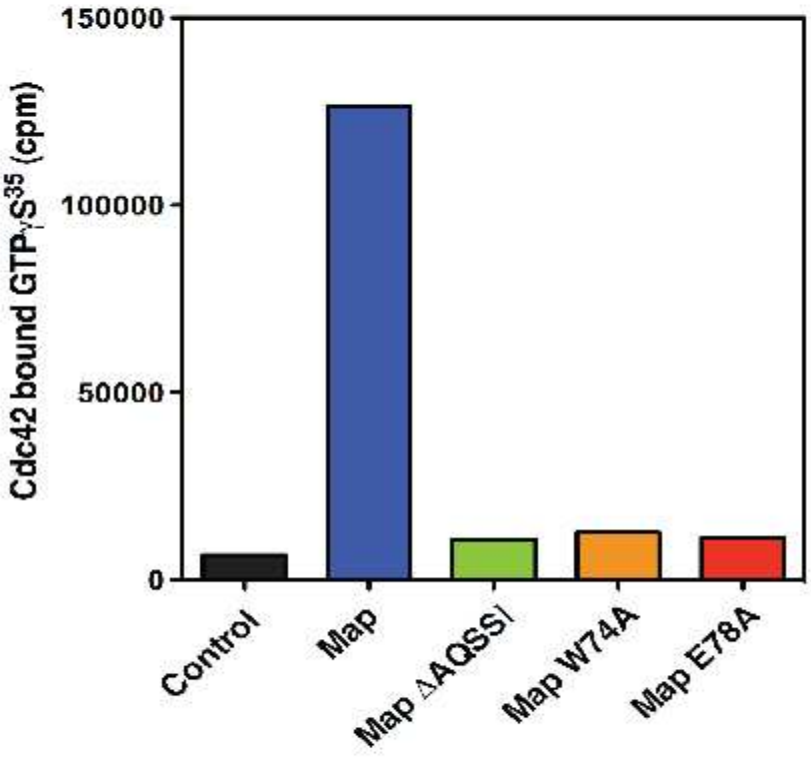
150000
100000
50000
0
Cdc42 bound GTPγS35 (cpm)
Control
Map
Map ΔAQSSI
Map W74A
Map E78A

FIGURE 21: WxxxE Motif and Putative Catalytic Loop are Necessary for Map Interaction with Cdc42 II. GST pull-down of 10ug nucleotide free GST-Cdc42 incubated with 20ug of control, MBP-Map, MBP-MapW74A, MBP-Map E78A, and MBP-MapΔAQSSI as indicated. SDS-PAGE gels stained with Coomassie Brilliant Blue were used to detect specific Cdc42 binding interactions.

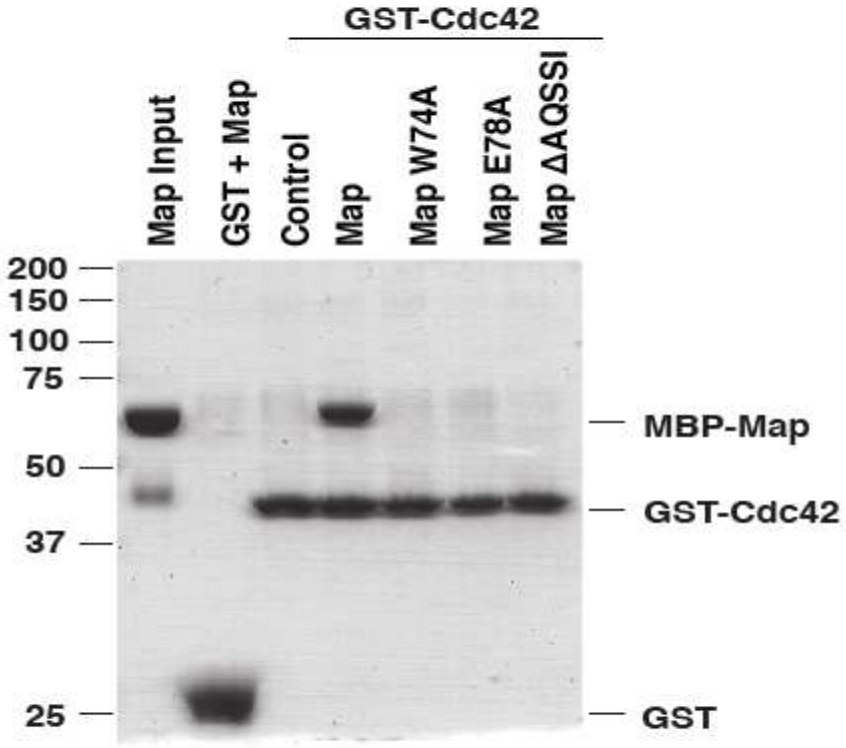
GST-Cdc42
Map Input
GST + Map
Control
Map
Map W74A
Map E78A
Map ΔAQSSI
200
150
100
75
50
37
25
MBP-Map
GST-Cdc42
GST

We had previously demonstrated that the invariant WxxxE residues are critical for the cellular actions of Map to induce cell surface filopodia, an actin phenotype ascribed to Cdc42. The local WxxxE environment appears to maintain the structural integrity and orientation of the putative α3-α4 catalytic loop (Figure 11). To test this idea, mutant Map W74A and E78A proteins were incubated with nucleotide free Cdc42 and assessed for protein binding. Neither mutant bound to Cdc42 *in vitro* (Figure 19). In addition, the WxxxE mutants had no GEF activity in either the GDP release (Figure 20) or guanine-nucleotide exchange assays (Figure 21). These finding lend further biochemical support to the notion that Map is a structural and functional homolog of SopE.

D. Map Functions as a GEF in human cells.

Type III secreted Map induces transient cell surface filopodia surrounding EPEC microcolonies via a Cdc42 dependent process (Kenny et al., 2002). While ectopic expression of Map in tissue culture cells recapitulates this phenotype (Alto et al., 2006), inhibitor studies suggested that Map signaling might be Cdc42 independent under these experimental conditions. Therefore, we set out to determine if the newly identified Cdc42 GEF activity is indeed required for filopodia generation in human cells. Transient transfection of the catalytic loop mutant MapΔAQSSI had not effect on the actin architecture whereas wild-type Map was a potent actin nucleator (Figure 22 and 23). Next, our findings using transiently transfected Map were directly compared to type III secreted Map in EPEC models of pathogenesis (Figure 23). As expected, filopodia were found surrounding 46±7.5% of EPEC microcolonies 30 minutes post infection. This phenotype was lost in the EPECΔ*map* strain (Figure 23). We examined the role of Cdc42

GEF activity by complementing Δ*map* strains of EPEC with plasmid expressed wild-type Map or MapΔAQSSI mutant (Figure 23). Type III delivery of wild-type Map produced transient filopodia in 60±4% of Hela cells whereas this phenotype was nearly undetectable by complementation with the GEF inactive MapΔAQSSI mutant (Figure 23). These findings clearly demonstrate a critical role of Map GEF in host cell actin filopodia production.

FIGURE 22: WxxxE Motif and Putative Catalytic Loop are Necessary to Induce Filopodia Phenotype. 293A cells transiently transfected with GFP-Map and the indicated mutant constructs were observed by direct fluorescence of rhodamine-phalloidin to detect F-actin (red). Arrows indicate transfected cells. Only wild-type Map induced cell surface filopodia. Performed by Sarah Sutton.

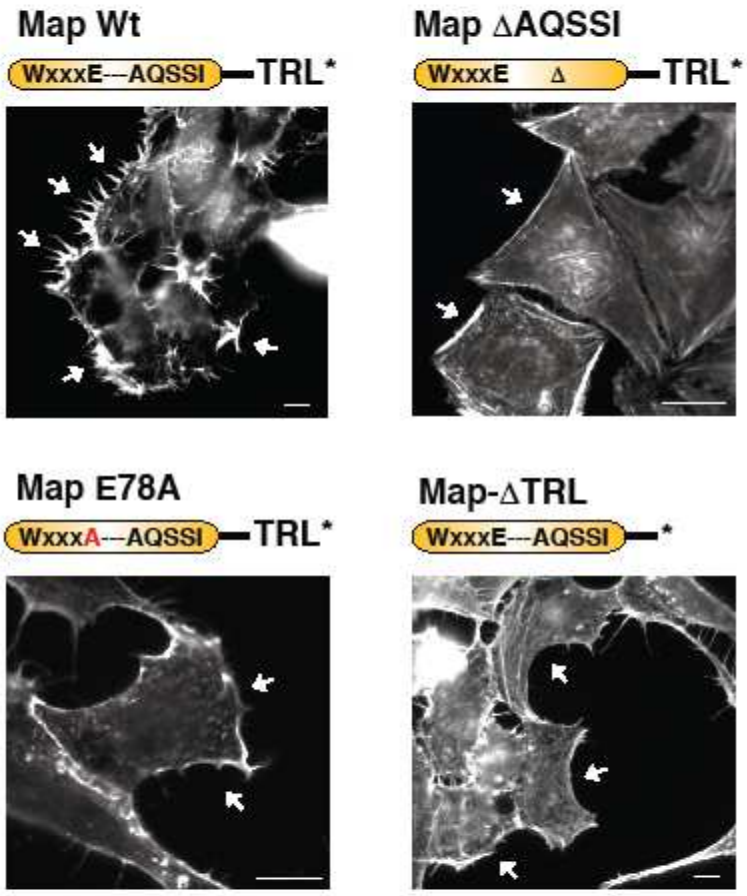
Map Wt
WxxxE---AQSSI
TRL*
Map ΔAQSSI
WxxxE Δ
TRL*
Map E78A
WxxxA---AQSSI
TRL*
Map-ΔTRL
WxxxE---AQSSI
*

FIGURE 23: Wild Type Map is Necessary for Filopodia Phenotype. Quantification of new actin filopodia in GFP-Map (92.3±3%) and GFP-MapΔAQSSI (3.7±1%) expressing cells after 18 hours of transfection (left). Pre-activated EPEC or EPECΔ*map* strains were incubated with HeLa cells for 30 minutes and assessed for actin filopodia by rhodamine-phalloidin. EPECΔ*map* strain was complemented with plasmid expressing wild-type Map (pMap) or mutant MapΔAQSSI (pMapΔAQSSI) as indicated. Performed by Sarah Sutton.

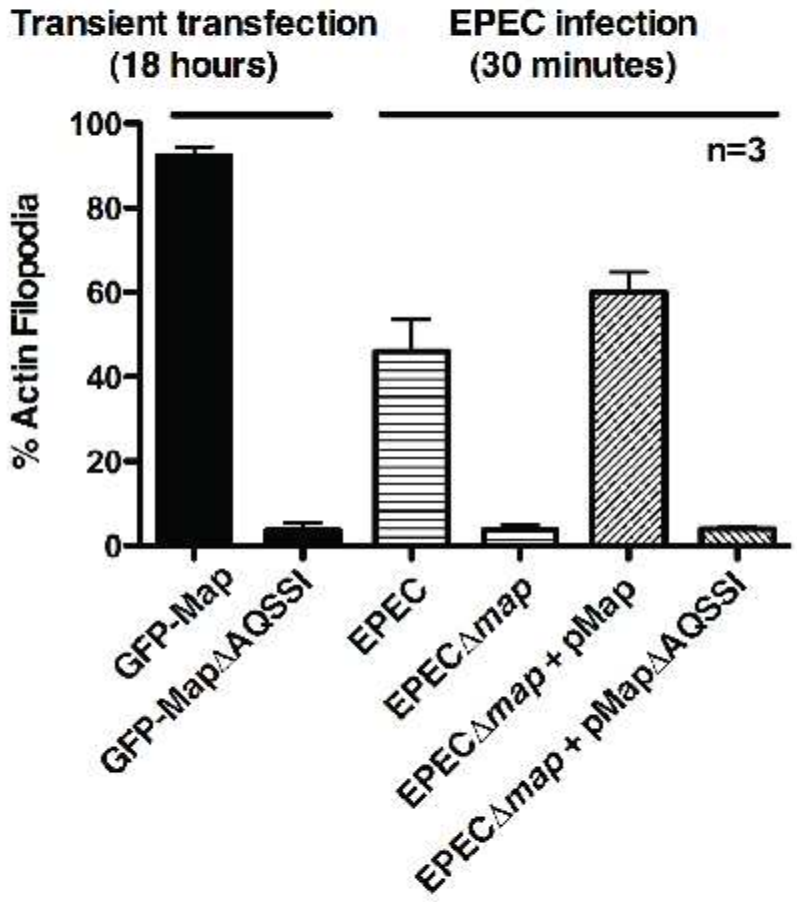
Transient transfection
(18 hours)
EPEC infection
(30 minutes)
n=3
% Actin Filopodia
100
80
60
40
20
0
GFP-Map
GFP-MapΔAQSSI
EPEC
EPECΔmap
EPECΔmap + pMap
EPECΔmap + pMapΔAQSSI

Recently our laboratory and others have shown that a C-terminal PSD-95/Dlg/Zo-1 (PDZ) ligand motif of Map is required for its signaling efficacy in cells (Alto et al., 2006; Simpson et al., 2006). The last three residues T-R-L in Map conform to the S/T-X-Ø consensus Type-I PDZ ligand and this sequence is identical to the PDZ motif of human CFTR (Short et al., 1998). As shown in Figure 22, exogenous expression GFP-Map induces robust filopodia formation whereas mutant DTRL Map protein has no effect. To determine if these changes in the C-terminus of Map compromised its catalytic activity, we performed *in vitro* Cdc42 GEF assays on whole cell-lysates expressing various GFP-Map mutants. MapDTRL maintained potent GEF activity *in vitro* whereas the GEF defective Map E78A mutant did not activate Cdc42 (Figure 24). We now propose a model in which *E. coli* induced filopodia requires a dual signaling mechanism involving Cdc42 activation coupled to a specific Epb50 subcomplex of currently unknown composition (Figure 25).

FIGURE 24: Map Functions as a GEF in human cells. *In vitro* Cdc42 GDP/GTP exchange assays using 293T cell lysates expressing GFP tagged version of Map and the indicated mutants. Exchange reactions were conducted with 1μM Cdc42 (GDP) in the presence of GTP□S^{35} for 10 minutes. Untreated cell extract controls were subtracted from each data point and the Ccdc42 GEF activity was normalized to GFP-Map activity of 100%. The average of three independent experiments and SEM are shown. Performed by Sarah Sutton.

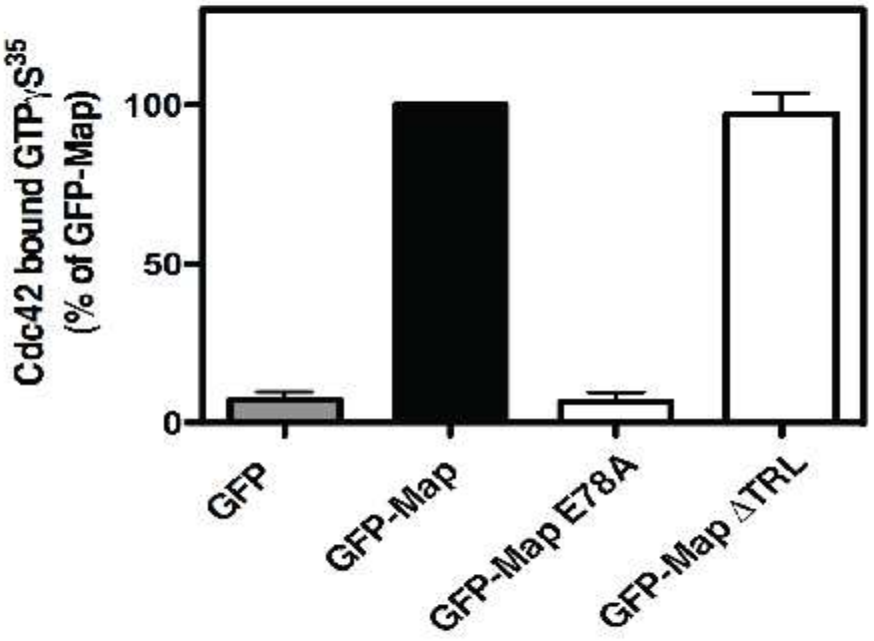
Cdc42 bound GTPγS35
(% of GFP-Map)
100
50
0
GFP
GFP-Map
GFP-Map E78A
GFP-Map ΔTRL

FIGURE 25: Diagram of Map signaling in human cells. Schematic depicting the behavior of Map in Cdc42 mediated signaling.

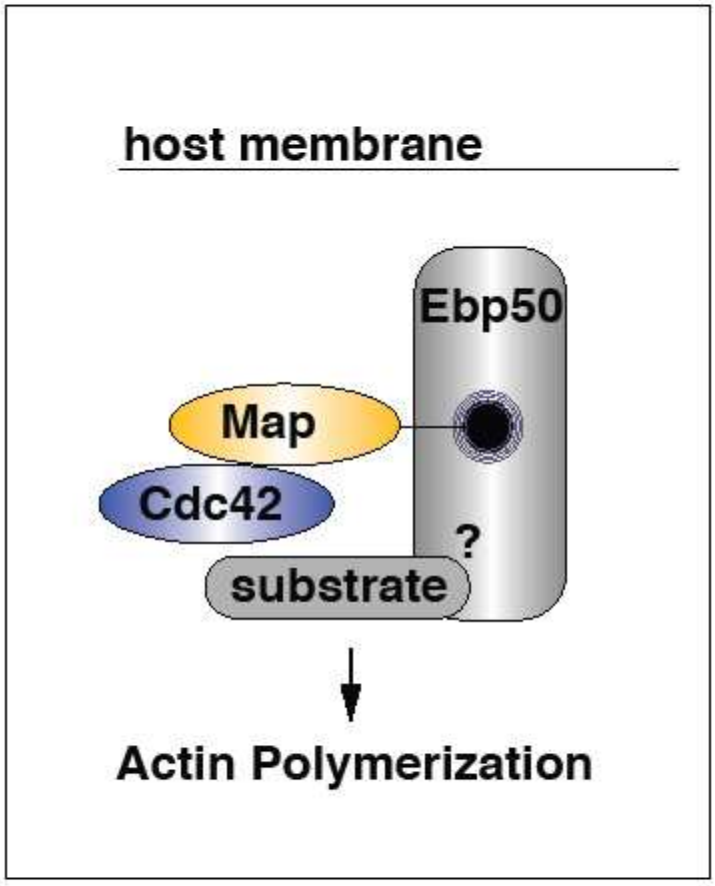
host membrane
Ebp50
Map
Cdc42
?
substrate
Actin Polymerization

CHAPTER 4. MATERIALS AND METHODS

A. Plasmids

The *map* gene from EHEC O157:H7 (accession #AP002566), IpgB2 from *S. flexneri* (accession # 13449076), and SifA from *S. typhimurium* LT2 (accession #AE008573) were PCR cloned in-frame into a modified 6x-His/MBP fusion vector with a pet28B backbone. Bacterial expression clones encoded residues 37-203 of Map, 20-188 of IpgB2, and either full-length or 133-336 of SifA. These constructs conferred soluble protein production and maintained the six helical SopE-like GEF fold. For mammalian expression, full-length *map* was subcloned into pEGFP-C2 (Clontech) using PCR. For stable transfection a TAP tagged (flag tag-TEV-Protein A sequence) *map* gene or control TAP tag alone was subcloned into pcDNA4T/O. All mutants were generated using a QuickChange™ Site-Directed Mutagenesis (Stratagene) kit following manufacturers instructions. CaaX chimeras were generated by PCR. All constructs were verified correct by sequencing.

B. Yeast Expression of IpgB2:

IpgB2 was PCR cloned into pENTR/D-TOPO (Invitrogen). Mutations were engineered by QuickChange™ Site-Directed Mutagenesis (Stratagene) of the IpgB2 template in pENTR/D-TOPO. Each mutations was confirmed by sequencing. Mutant IpgB2 constructs were Gateway recombined into pYes-DEST52 (Invitrogen), a yeast expression vector with a *GAL1* galactose inducible promoter and a URA3 selectable marker. pYes-Dest52 plasmids were transformed using the standard lithium acetate method into the yeast strain InvSc1: *MATα his3D1 leu2 trp1-289 ura3-52 his3D1 leu2 trp1-289 ura3-52* (Invitrogen). Transformants were selected for by

plating on synthetic dextrose medium minus Uracil (SD-Ura) with 20% glucose for three days at 30°C. Single colonies were streaked onto SD-Ura with 10% galactose and 10% rafinose for two to three days at 30°C to induce IpgB2 expression. Plates were then assayed for mutant growth phenotypes.

C. Protein expression and purification:

6xHis/MBP-Map, IpgB2, and SifA were expressed in *E. coli* BL21 (DE3) cells using 0.4 mM isopropyl-beta-D-thiogalactopyranoside (IPTG) for 18 hours at 16°C. Cells were pelleted, resuspended in TBS/DTT buffer [Tris buffered saline (TBS) with 1 mM dithiothreitol (DTT) and complete EDTA-free protease inhibitor tablets (Roche)], emulsiflexed on ice three times, and clarified by centrifugation at 14K for 30 minutes at 4°C. 6xHis/MBP proteins were purified on Ni-NTA beads following the manufacturers instructions (Qiagen). 1ml of proteins were injected into a 24 ml bed volume sephadex-75 column interfaced to an AKTA FPLC (Amersham) and 1ml elution fractions were collected. Fractions containing the desired protein were detected by spectrophotometric analysis (280 nm) and SDS-PAGE, collected and concentrated. GST-tagged Rho GTPases were purified on glutathione-sepharose beads as previously described (Self and Hall, 1995).

D. GST pulldown and GEF assays:

For GST pulldown assays, Glutathione sepharose beads (25 µl) were incubated with 10µg GST-RhoA, Rac1, or Cdc42 and stripped of nucleotide by incubating beads with TBS/DTT and 10mM

EDTA. GTPases were washed in TBS containing 1mM EDTA and 1% Triton-X 100. 10μg of WxxxE bacterial proteins were incubated with the GTPases for 1 hour at 4° and washed 3 times with TBS/DTT Triton buffer. Protein interactions were analyzed by SDS-PAGE and Coomassie stained proteins. GEF assays were conducted as reported (Zheng et al., 1995). Cellular supernatants for these assays were prepared from transiently transfected 293T cells expressing GFP-tagged Map and the indicated mutants. Plasmids for transient transfection were purified using the Endo-free Maxi kit (Qiagen) and transfected into 293T cells using FuGENE6 (Roche) according to manufacturers instructions. Extracts were prepared by lysing cells with 20mM Tris 7.4,100 mM NaCl, 1mM EDTA, 10 mM $MgCl_2$ and 0.5% Triton-X 100 and clarification by centrifugation at 14K for 15 minutes at 4°C.

E. EPEC infection and indirect immunofluorescence

Wild-type EPEC E2348/69 and EPECΔ*map* strains were obtained from Dr. Brendan Kenny (Kenny and Jepson, 2000). Complementation plasmid pBBR1MCS1 carrying the *map* or *map□AQSSI* gene was introduced into EPECΔ*map* strain (B. Kenny) by electroporation. HeLa cells were infected with EPEC strains for 30 minutes with pre-activated EPEC as described previously(Kenny et al., 2002). GFP-Map and mutant transfected cells were processed and stained as previously described (Alto et al., 2007). Briefly, cells fixed and then stained with Rhodamine-phalloidin to detect cellular actin. Microscopy was performed on a Zeiss Axiovert microscope (Carl Zeiss Microimaging, Inc.) using a MicroMax digital camera (Roper-Princeton Instruments) controlled by MetaFluor software (Universal Imaging, Corp.). Optical filters were obtained from Chroma Technologies and 40x or 63x objectives were used for image acquisition.

CHAPTER 5. DISCUSSION

We have identified the first enzymatic activity for one member of a large type III effector family expressed by *E. coli*, *Salmonella* and *Shigella* species. *E. coli* Map displays potently and specifically enhances guanine-nucleotide exchange on human GTPase Cdc42. We also present several lines of evidence in support of the observation that WxxxE effectors adopt a functional SopE-like GEF structure and these type III effectors may directly couple Rho GTPase activation to downstream signaling pathways via a dual signaling mechanism. Together, these findings have revealed a highly sophisticated form of information transfer from bacterial pathogens to the actin cytoskeletal regulatory machinery of the host cell.

A. The SopE/SifA structure represents an adaptable scaffold for the evolution of pathogenic GEFs.

The atomic structure of C-terminal SifA resembles the *Salmonella* GEF type III effector SopE (*Ohlson et al., 2008*). However, no GEF activity for SifA has been demonstrated and it was unclear if any of the WxxxE-containing type III effectors displayed a SopE-like structure or had GEF activity. Three lines evidence support the role of WxxxE effectors as SopE-like GEFs. First, we could accurately predict conserved residues and functional motifs in the *Shigella* WxxxE effector IpgB2 from the structural analogy to the SopE*Cdc42 complex. Second, we found that the EHEC O157:H7 Map is a potent GEF for Cdc42 *in vitro*, the first demonstration of such activity for any WxxxE type III effector family-member. Third, Map appeared to use a SopE-like mechanism as deletion of the putative catalytic loop region abolished Cdc42 activation *in vitro* and in cells. Because conserved protein regions and structural motifs are critical for

bacterial activation of Rho GTPase signaling pathways by Map, IpgB1, IpgB2 (*10)*, SifA (*Ohlson et al., 2008*) and numerous other WxxxE-containing type III effectors (Alto et al., 2006; Arbeloa et al., 2008) it is likely that all of the family members display SopE-like structure and/or GEF activity.

Are all WxxxE effectors GEFs? It was surprising to find that neither *Shigella* IpgB2 nor *Salmonella* SifA induced significant guanine-nucleotide exchange on recombinant RhoA even though these WxxxE type III effectors utilize RhoA signaling pathways to facilitate bacterial pathogenesis (*Ohlson et al. 2008*) (Alto et al., 2006). These results may be due to our experimental conditions in which the appropriate prenylation of GTPases or additional post-translational modifications of the type III effectors are necessary for their binding interactions *in vitro*. Alternatively, additional co-factors may be required to activate the bacterial GEFs. These factors may include host proteins or additional type III effector proteins secreted during infection. This appears to be the case for SifA, which nucleates a multivalent complex composed of host SKIP and RhoA as well as the type III effector SseJ at the *Salmonella* containing vacuole (*Ohlson et al, 2008*). Further studies will be needed to delineate the GEF activity of WxxxE effectors to downstream signaling outputs in host cells.

B. WxxxE effectors couple Rho GTPase activation to downstream signaling cascades.

Our laboratory previously suggested that the WxxxE effectors mimic host Rho GTPases despite the fact that these bacterial proteins have no sequence homology, secondary structural similarities, or bind guanine-nucleotides similar to the GTPases (Alto et al., 2006). The evidence in support of this hypothesis was that WxxxE effectors, such as Map, activate actin

polymerization events in the presence of the GTPase inhibitor YopT. In contrast, inhibition of downstream targets of GTPases such as N-WASP blocked Map activity. Furthermore, the two *Shigella* WxxxE effectors IpgB1 and IpgB2 were shown to interact with GTPase substrates Elmo/DOCK180 (Handa et al., 2007) and ROCK/mDia1 (Alto et al., 2006) respectively in the presence of whole cell lysates. From the structural and biochemical evidence presented here, we now conclude that at least one WxxxE effector can function upstream of the GTPases as a GEF. Map displays potent and highly specific GEF activity for Cdc42 *in vitro* and disruption of protein motifs that are predicted to be involved in Cdc42 exchange catalysis disrupt the actin polymerization capabilities of Map in human cells. Can these two models, GTPase mimicry or GEF activity, be reconciled through a more sophisticated signaling mechanism than originally proposed?

The data presented in this report in conjunction with previous work from our laboratory and that of Simpson et al. supports a highly sophisticated signaling mechanism for *E. coli* Map (Alto et al., 2006; Simpson et al., 2006). In addition to its SopE-like GEF domain, Map harbors a PDZ (PSD-95/Dlg/ZO-1) interaction motif at its C-terminus. This motif in Map binds directly to the PDZ protein Ebp50, an apically localized scaffold that couples ion channels and transporters to the actin cytoskeleton. A deletion of the C-terminal PDZ interaction motif, or siRNA knockdown of Ebp50, inhibits actin polymerization induced by Map (Alto et al., 2006; Simpson et al., 2006).

Approximately 37% of human GEF proteins (26/70) have PDZ ligands at their C-terminus (Garcia-Mata and Burridge, 2007). These motifs are thought to dictate GTPase signaling specifity by coupling Rho proteins directly to their downstream effector substrates (Garcia-Mata and Burridge, 2007). In fact, the nucleation of a GTPase/effector complex by

GEFs is a physiologically relevant signaling mechanism in human cells. An excellent example of this phenomenon was originally reported by Manser *et al.* in which the GEF β-Pix (also called Cool-1 or ArhGEF7) nucleates a complex between Rac1 or Cdc42 and its effector substrate p21 activated kinase (PAK) (Manser et al., 1998). This GEF/GTPase/effector complex is required to spatially orient migrating neutrophils towards an asymmetrical chemoattractant gradient (Li et al., 2003).

It seems likely that compartmentalization of Map GEF activity into a specific Epb50 complex can demarcate filopodia-specific actin signals from the multitude of actin signaling pathways induced by EPEC type III effectors. While Map directly activates Cdc42 through a SopE-like GEF mechanism (shown in this study), the type III effectors Tir and EspFu induce actin-rich pedestals beneath bacterial microcolonies in a Cdc42 independent manner (Ben-Ami et al., 1998; Campellone et al., 2004). Tir indirectly activates N-WASP, a downstream Cdc42 substrate (Gruenheid et al., 2001; Kalman et al., 1999). In addition, EspFu and EspF directly regulates N-WASP activity by physically displacing an autoinhibitory domain (Alto et al., 2007; Cheng et al., 2008; Sallee et al., 2008). It is intriguing to speculate that *E. coli* Map nucleates new GTPase/effector signaling complexes that is specifically tuned to an infectious disease output. In essence, Map would buffer Cdc42 activation and downstream signaling form other type III effector pathways. Map is localized to mitochondria (Kenny and Jepson, 2000) and it also functions at tight junctions to disrupt the intestinal permeability barrier (Dean and Kenny, 2004). It will be intriguing to determine if Cdc42 is activated at these sites by Map as it has been implicated in signaling within these subcellular domains

Map is not the only WxxxE effector that couples GTPases to additional host substrates. Recently, Ohlson *et al.* proposed that *Salmonella* SifA regulates host membrane trafficking by

directly associating with the GTPase RhoA. Surprisingly however, SifA does not induce actin polymerization or stress fiber formation, two phenotypes directly linked to RhoA function. One interpretation of this data is that SifA does not activate RhoA but simply binds the GTPase and localizes it to the *Salmonella* containing vacuole. In contrast, it is also possible that SifA couples RhoA to a specific set of substrates that regulates membrane trafficking but not actin dynamics. In support of this idea, it was recently shown that SKIP interacts with the GTPase Rab9 and that SifA antagonizes the SKIP/Rab9 interaction (Jackson et al., 2008). Therefore, the coordination between bacterial type III effectors, GTPases, and their down stream substrates could be a major signaling mechanism of numerous infectious disease agents.

C. EspH as a possible negative regulator.

The possibility that the WxxxE family may be GEFs raises the inevitable question of whether there are any corollary effectors or effector groups behaving in an inhibiting manner, such as a GAP. There is precedent for such a scenario. The *Salmonella* effectors SopE and SptP function as GEF and GAP respectively during infection. SopE activates Rac1 allowing the formation of lamellipodia and the engulfment of the *Salmonella* vacuole while SptP inactivates Rac1 in an effort to evade immune detection by returning the apical epithelial surface to its original state (Donnenberg *et al*., 1999). Another LEE encoded effector seems to be a good candidate for a negative regulator of Map. EspH appears to be the anti-Map in that it inhibits filipodia formation while promoting pedestal formation and produces a rounding phenotype in transfected cells (Tu et al., 2003). Preliminary examination of EspH with GTPase assays and lysate pulldown experiments seems to indicate that it is not a GAP or interacting with RhoA,

Rac1, or Cdc42 (Figure 25). The protein is localized to the cellular membrane during infection (Tu et al. 2003) so the possibility exists that is behaving like YopT or YpkA by removing lipid modifications or otherwise displacing GTPases like Cdc42. Regardless of the final verdict for EspH, it is likely that pathogens have evolved negative regulators to counter and restrain the activity of their WxxxE effectors.

Figure 26: EspH does not Interact with Active RhoA, Rac1, or Cdc42. Pulldown experiment of lysate from transfected HEK293T with 30 μg of GST-tagged, constitutively active mutants of RhoA (), Rac1 (), and Cdc42 () and using GST as a control. EspH has a molecular weight just under 20 kD. The band above 25 kD is a nonspecific artifact.

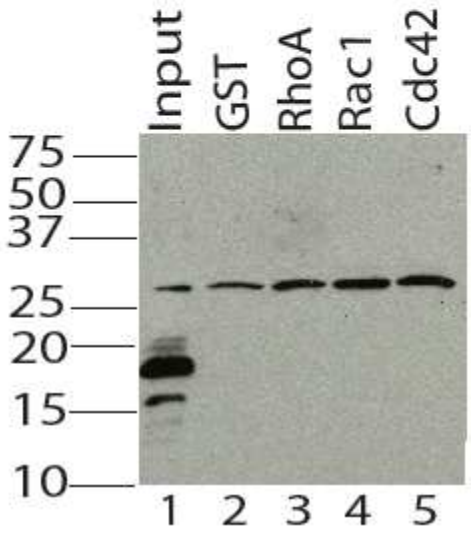
Input
GST
RhoA
Rac1
Cdc42
75
50
37
25
20
15
10
1
2
3
4
5

BIBLIOGRAPHY

Aktories, K., and Hall, A. (1989) Botulinum ADP-ribosyltransferase C3: a new tool to study low molecular weight GTP-binding proteins. Trends Pharmacol Sci *10* 415–418.

Alto, N.M. (2008) Mimicking small G-proteins: an emerging theme from bacterial virulence arsenal. Cellular Microbiology *10*, 566-575.

Alto, N.M., Shao, F., Lazar, C.S., Brost, R.L., Chua, G., Mattoo, S., McMahon, S.A., Ghosh, P., Hughes, T.R., Boone, C., and Dixon, J.E. (2006). Identification of a bacterial type III effector family with G protein mimicry functions. Cell *124*, 133-145.

Alto, N.M., Weflen, A.W., Rardin, M.J., Yarar, D., Lazar, C.S., Tonikian, R., Koller, A., Taylor, S.S., Boone, C., Sidhu, S.S*., et al.* (2007). The type III effector EspF coordinates membrane trafficking by the spatiotemporal activation of two eukaryotic signaling pathways. The Journal of cell biology *178*, 1265-1278.

Arbeloa, A., Bulgin, R.R., MacKenzie, G., Shaw, R.K., Pallen, M.J., Crepin, V.F., Berger, C.N., and Frankel, G. (2008). Subversion of actin dynamics by EspM effectors of attaching and effacing bacterial pathogens. Cellular microbiology *10*, 1429-1441.

Ben-Ami, G., Ozeri, V., Hanski, E., Hofmann, F., Aktories, K., Hahn, K.M., Bokoch, G.M., and Rosenshine, I. (1998). Agents that inhibit Rho, Rac, and Cdc42 do not block formation of actin pedestals in HeLa cells infected with enteropathogenic Escherichia coli. Infection and immunity *66*, 1755-1758.

Beuzon, C.R., Meresse, S., Unsworth, K.E., Ruiz-Albert, J., Garvis, S., Waterman, S.R., Ryder, T.A., Boucrot, E., and Holden, D.W. (2000). Salmonella maintains the integrity of its intracellular vacuole through the action of SifA. The EMBO journal *19*, 3235-3249.

Boucrot, E., Beuzon, C.R., Holden, D.W., Gorvel, J.P., and Meresse, S. (2003) Salmonella typhimurium SifA effector protein requires its membrane-anchoring C-terminal hexapeptide for its biological function. J Biol Chem *278*, 14196–14202.

Bretscher, A., Chambers, D., Nguyen, R., and Reczek, D. (2000) ERM-Merlin and EBP50 protein families in plasma membrane organization and function. Annu Rev Cell Dev Biol *16*, 113–143.

Brumell, J.H., Goosney, D.L., and Finlay, B.B. (2002) SifA, a type III secreted effector of Salmonella typhimurium, directs Salmonella-induced filament (Sif) formation along microtubules. Traffic *3*, 407–415.

Buchwald, G., Friebel, A., Galan, J.E., Hardt, W.D., Wittinghofer, A., and Scheffzek, K. (2002). Structural basis for the reversible activation of a Rho protein by the bacterial toxin SopE. The EMBO journal *21*, 3286-3295.

Campellone, K.G., Robbins, D., and Leong, J.M. (2004). EspFU is a translocated EHEC effector that interacts with Tir and N-WASP and promotes Nck-independent actin assembly. Dev Cell *7*, 217-228.

Cheng, H.C., Skehan, B.M., Campellone, K.G., Leong, J.M., and Rosen, M.K. (2008). Structural mechanism of WASP activation by the enterohaemorrhagic E. coli effector EspF(U). Nature *454*, 1009-1013.

Colicelli, J. (2004) Human RAS superfamily proteins and related GTPases. Sci STKE 2004: RE13.

Dean, P., and Kenny, B. (2004). Intestinal barrier dysfunction by enteropathogenic Escherichia coli is mediated by two effector molecules and a bacterial surface protein. Molecular microbiology *54*, 665-675.

Donnenberg, M.S. (1999) Microbiology: Salmonella strikes a balance. Nature *401*, 218-219.

Flatau, G., Lemichez, E., Gauthier, M., Chardin, P., Paris, S., Fiorentini, C., and Boquet, P. (1997) Toxin-induced activation of the G protein p21 Rho by deamidation of glutamine. Nature *387*, 729–733.

Fu, Y., and Galan, J.E. (1999) A salmonella protein antagonizes Rac-1 and Cdc42 to mediate host-cell recovery after bacterial invasion. Nature *401*, 293–297.

Galan, J.E. (2001). Salmonella interactions with host cells: type III secretion at work. Annu Rev Cell Dev Biol *17*, 53-86.

Garcia-Mata, R., and Burridge, K. (2007). Catching a GEF by its tail. Trends in cell biology *17*, 36-43.Garmendia, J., Phillips, A.D., Carlier, M.F., Chong, Y., Schuller, S., Marches, O., Dahan, S., Oswald, E., Shaw, R.K., Knutton, S., and Frankel, G. (2004). TccP is an enterohaemorrhagic Escherichia coli O157:H7 type III effector protein that couples Tir to the actin-cytoskeleton. Cellular microbiology *6*, 1167-1183.

Gruenheid, S., DeVinney, R., Bladt, F., Goosney, D., Gelkop, S., Gish, G.D., Pawson, T., and Finlay, B.B. (2001). Enteropathogenic E. coli Tir binds Nck to initiate actin pedestal formation in host cells. Nature cell biology *3*, 856-859.

Gruenheid, S., Sekirov, I., Thomas, N.A., Deng, W., O'Donnell, P., Goode, D., Li, Y., Frey, E.A., Brown, N.F., Metalnikov, P.*, et al.* (2004). Identification and characterization of NleA, a non-LEE-encoded type III translocated virulence factor of enterohaemorrhagic Escherichia coli O157:H7. Molecular microbiology *51*, 1233-1249.

Hachani, A., Biskri, L., Rossi, G., Marty, A., Menard, R., Sansonetti, P., Parsot, C., Van Nhieu, G.T., Bernardini, M.L., and Allaoui, A. (2008). IpgB1 and IpgB2, two homologous effectors secreted via the Mxi-Spa type III secretion apparatus, cooperate to mediate polarized cell invasion and inflammatory potential of Shigella flexenri. Microbes and infection / Institut Pasteur *10*, 260-268.

Hall, A. (1998) Rho GTPases and the actin cytoskeleton. Science *279*, 509–514.

Handa, Y., Suzuki, M., Ohya, K., Iwai, H., Ishijima, N., Koleske, A.J., Fukui, Y., and Sasakawa, C. (2007). Shigella IpgB1 promotes bacterial entry through the ELMO-Dock180 machinery. Nature cell biology *9*, 121-128.

Hardt, W.D., Chen, L.M., Schuebel, K.E., Bustelo, X.R., and Galan, J.E. (1998). S. typhimurium encodes an activator of Rho GTPases that induces membrane ruffling and nuclear responses in host cells. Cell *93*, 815-826.

Hart, M.J., Eva, A., Evans, T., Aaronson, S.A., and Cerione, R.A. (1991). Catalysis of guanine nucleotide exchange on the CDC42Hs protein by the dbl oncogene product. Nature *354*, 311-314.

Harvey, J.J. (1964) An unidentified virus which causes the rapid production of tumours in mice. Nature *204*, 1104–1105.

Ingmundson, A., Delprato, A., Lambright, D.G., and Roy, C.R. (2007) Legionella pneumophila proteins that regulate Rab1 membrane cycling. Nature *450*, 365–369.

Jackson, L.K., Nawabi, P., Hentea, C., Roark, E.A., and Haldar, K. (2008). The Salmonella virulence protein SifA is a G protein antagonist. Proceedings of the National Academy of Sciences of the United States of America *105*, 14141-14146.

Jaffe, A.B., and Hall, A. (2005) Rho GTPases: biochemistry and biology. Annu Rev Cell Dev Biol *21*, 247–269.

Kalman, D., Weiner, O.D., Goosney, D.L., Sedat, J.W., Finlay, B.B., Abo, A., and Bishop, J.M. (1999). Enteropathogenic E. coli acts through WASP and Arp2/3 complex to form actin pedestals. Nature cell biology *1*, 389-391.

Katoh, H., and Negishi, M. (2003) RhoG activates Rac1 by direct interaction with the Dock180-binding protein Elmo. Nature *424*, 461–464.

Kelly, M., Hart, E., Mundy, R., Marches, O., Wiles, S., Badea, L., Luck, S., Tauschek, M., Frankel, G., Robins-Browne, R.M., and Hartland, E.L. (2006). Essential role of the type III secretion system effector NleB in colonization of mice by Citrobacter rodentium. Infection and immunity *74*, 2328-2337.

Kenny, B., Ellis, S., Leard, A.D., Warawa, J., Mellor, H., and Jepson, M.A. (2002). Co-ordinate regulation of distinct host cell signalling pathways by multifunctional enteropathogenic Escherichia coli effector molecules. Molecular microbiology *44*, 1095-1107.

Kenny, B., and Jepson, M. (2000). Targeting of an enteropathogenic Escherichia coli (EPEC) effector protein to host mitochondria. Cellular microbiology *2*, 579-590.

Kenny, B., Ellis, S., Leard, A.D., Warawa, J., Mellor, H., and Jepson, M.A. (2002) Co-ordinate regulation of distinct host cell signalling pathways by multifunctional enteropathogenic Escherichia coli effector molecules. Mol Microbiol *44*, 1095–1107.

Kirsten, W.H., and Mayer, L.A. (1969) Malignant lymphomas of extrathymic origin induced in rats by murine erythroblastosis virus. J Natl Cancer Inst *43*, 735–746.

Li, Z., Hannigan, M., Mo, Z., Liu, B., Lu, W., Wu, Y., Smrcka, A.V., Wu, G., Li, L., Liu, M.*, et al.* (2003). Directional sensing requires G beta gamma-mediated PAK1 and PIX alpha-dependent activation of Cdc42. Cell *114*, 215-227.

Lommel, S., Benesch, S., Rottner, K., Franz, T., Wehland, J., and Kuhn, R. (2001) Actin pedestal formation by enteropathogenic Escherichia coli and intracellular motility of Shigella flexneri are abolished in N-WASP-defective cells. EMBO Rep *2*, 850–857.

Manser, E., Loo, T.H., Koh, C.G., Zhao, Z.S., Chen, X.Q., Tan, L., Tan, I., Leung, T., and Lim, L. (1998). PAK kinases are directly coupled to the PIX family of nucleotide exchange factors. Molecular cell *1*, 183-192.

Marches, O., Wiles, S., Dziva, F., La Ragione, R.M., Schuller, S., Best, A., Phillips, A.D., Hartland, E.L., Woodward, M.J., Stevens, M.P., and Frankel, G. (2005). Characterization of two non-locus of enterocyte effacement-encoded type III-translocated effectors, NleC and NleD, in attaching and effacing pathogens. Infection and immunity *73*, 8411-8417.

McDaniel, T.K., Jarvis, K.G., Donnenberg, M.S., and Kaper, J.B. (1995). A genetic locus of enterocyte effacement conserved among diverse enterobacterial pathogens. Proceedings of the National Academy of Sciences of the United States of America *92*, 1664-1668.

Moon, H.W., Whipp, S.C., Argenzio, R.A., Levine, M.M., and Giannella, R.A. (1983) Attaching and effacing activities of rabbit and human enteropathogenic Escherichia coli in pig and rabbit intestines. Infect Immun *41*, 1340–1351.

Ohya, K., Handa, Y., Ogawa, M., Suzuki, M., and Sasakawa, C. (2005) IpgB1 is a novel shigella effector protein involved in bacterial invasion of host cells: its activity to promote membrane ruffling via RAC1 and CDC42 activation. J Biol Chem *280*, 24022–24034.

Nagai, H., Kagan, J.C., Zhu, X., Kahn, R.A., and Roy, C.R. (2002) A bacterial guanine nucleotide exchange factor activates ARF on Legionella phagosomes. Science *295*, 679–682.

Ohya, K., Handa, Y., Ogawa, M., Suzuki, M., and Sasakawa, C. (2005). IpgB1 Is a Novel Shigella Effector Protein Involved in Bacterial Invasion of Host Cells: ITS ACTIVITY TO PROMOTE MEMBRANE RUFFLING VIA RAC1 AND CDC42 ACTIVATION. The Journal of biological chemistry *280*, 24022-24034.

Pawson, T., and Scott, J.D. (1997) Signaling through scaffold, anchoring, and adaptor proteins. Science *278*, 2075–2080.

Pederson, K.J., Vallis, A.J., Aktories, K., Frank, D.W., and Barbieri, J.T. (1999) The amino-terminal domain of Pseudomonas aeruginosa ExoS disrupts actin filaments via small-molecular-weight GTP-binding proteins. Mol Microbiol *32*, 393–401.

Phalipon, A., and Sansonetti, P.J. (2007). Shigella's ways of manipulating the host intestinal innate and adaptive immune system: a tool box for survival? Immunology and cell biology *85*, 119-129.

Prehna, G., Ivanov, M.I., Bliska, J.B., and Stebbins, C.E. (2006) Yersinia virulence depends on mimicry of host Rho-family nucleotide dissociation inhibitors. Cell *126*, 869–880.

Rossman, K.L., Worthylake, D.K., Snyder, J.T., Siderovski, D.P., Campbell, S.L., and Sondek, J. (2002). A crystallographic view of interactions between Dbs and Cdc42: PH domain-assisted guanine nucleotide exchange. The EMBO journal *21*, 1315-1326.

Sallee, N.A., Rivera, G.M., Dueber, J.E., Vasilescu, D., Mullins, R.D., Mayer, B.J., and Lim, W.A. (2008). The pathogen protein EspF(U) hijacks actin polymerization using mimicry and multivalency. Nature *454*, 1005-1008.

Schlumberger, M.C., Friebel, A., Buchwald, G., Scheffzek, K., Wittinghofer, A., and Hardt, W.D. (2003). Amino acids of the bacterial toxin SopE involved in G nucleotide exchange on Cdc42. The Journal of biological chemistry *278*, 27149-27159.

Schmidt, G., Sehr, P., Wilm, M., Selzer, J., Mann, M., and Aktories, K. (1997) Gln 63 of Rho is deamidated by Escherichia coli cytotoxic necrotizing factor-1. Nature *387*, 725–729.

Self, A.J., and Hall, A. (1995). Purification of recombinant Rho/Rac/G25K from Escherichia coli. Methods in enzymology *256*, 3-10.

Shao, F., Merritt, P.M., Bao, Z., Innes, R.W., and Dixon, J.E. (2002) A Yersinia effector and a Pseudomonas avirulence protein define a family of cysteine proteases functioning in bacterial pathogenesis. Cell *109*, 575–588.

Short, D.B., Trotter, K.W., Reczek, D., Kreda, S.M., Bretscher, A., Boucher, R.C., Stutts, M.J., and Milgram, S.L. (1998). An apical PDZ protein anchors the cystic fibrosis transmembrane conductance regulator to the cytoskeleton. The Journal of biological chemistry *273*, 19797-19801.

Simpson, N., Shaw, R., Crepin, V.F., Mundy, R., FitzGerald, A.J., Cummings, N., Straatman-Iwanowska, A., Connerton, I., Knutton, S., and Frankel, G. (2006). The enteropathogenic Escherichia coli type III secretion system effector Map binds EBP50/NHERF1: implication for cell signalling and diarrhoea. Molecular microbiology *60*, 349-363.

Songyang, Z., Fanning, A.S., Fu, C., Xu, J., Marfatia, S.M., Chishti, A.H., et al. (1997) Recognition of unique carboxyl-terminal motifs by distinct PDZ domains. Science *275*, 73–77.

Snapper, S.B., Takeshima, F., Anton, I., Liu, C.H., Thomas, S.M., Nguyen, D., et al. (2001) N-WASP deficiency reveals distinct pathways for cell surface projections and microbial actin-based motility. Nat Cell Biol *3*, 897–904.

Stein, M.A., Leung, K.Y., Zwick, M., Garcia-del Portillo, F., and Finlay, B.B. (1996). Identification of a Salmonella virulence gene required for formation of filamentous structures containing lysosomal membrane glycoproteins within epithelial cells. Molecular microbiology *20*, 151-164.

Tobe, T., Beatson, S.A., Taniguchi, H., Abe, H., Bailey, C.M., Fivian, A., Younis, R., Matthews, S., Marches, O., Frankel, G.*, et al.* (2006). An extensive repertoire of type III secretion effectors in Escherichia coli O157 and the role of lambdoid phages in their dissemination. Proceedings of the National Academy of Sciences of the United States of America *103*, 14941-14946.

Takai, Y., Sasaki, T., and Matozaki, T. (2001) Small GTP-binding proteins. Physiol Rev *81*, 153–208.

Von Pawel-Rammingen, U., Telepnev, M.V., Schmidt, G., Aktories, K., Wolf-Watz, H., and Rosqvist, R. (2000) GAP activity of the Yersinia YopE cytotoxin specifically targets the Rho pathway: a mechanism for disruption of actin microfilament structure. Mol Microbiol *36*, 737–748.

Worthylake, D.K., Rossman, K.L., and Sondek, J. (2000). Crystal structure of Rac1 in complex with the guanine nucleotide exchange region of Tiam1. Nature *408*, 682-688.

Zheng, Y., Hart, M.J., and Cerione, R.A. (1995). Guanine nucleotide exchange catalyzed by dbl oncogene product. Methods in enzymology *256*, 77-84.